Beamline BM08-LISA:
2020-2024 activity Report

LISA

Linea Italiana di Spettroscopia
di Assorbimento x

Authors: F. d’Acapito, S. Amatori, J. Orsilli and A. Puri

DOI: 10.5281/zenodo.15533084

Contents

Abbreviations

BLC: Beam-Line Commissioning.
BLISS: BeamLine Instrumentation Support Software.
BM: Bending Magnet.
CECOMEC: CEria-based COMpounds as effective catalyst for Electrochemical Cells.
CERIC: Central European Research Infrastructure Consortium.
CNR: Consiglio Nazionale delle Ricerche.
CRG: Collaborating Research Group.
DAC: Diamond Anvil Cell.
DOI: Digital Object Identifier.
EBS: Extremely Brilliant Source.
EH: Experimental Hutch.
ERIC: European Research Infrastructure Consortium.
ESRF: European Synchrotron Radiation Facility.
EXAFS: Extended X-ray Absorption Fine Structure.
FEXRAV: Fixed Energy Ray Absorption Voltammetry.
FY: Fluorescence Yield.
GILDA: General purpose Italian beamline for x-ray Diffraction and Absorption.
GIXAS: Grazing Incidence X-ray Absorption Spectroscopy.
GST: GeSbTe.
HER: Hydrogen evolution Reaction.
HERFD: High Energy Resolution Fluorescence Detection.
HPGe: High Purity Germanium.
IC: Ion Chamber.
IHR: In-House Research.
IOM: Istituto Officina dei Materiali.
iPCRAM: interface Phase Change Random access Memory.
KB : Kirkpatrick- Baez.
LCF: Linear Combination Fitting.
LISA: Linea Italiana per la Spettroscopia di Assorbimento di raggi X.
LN$_2$: Liquid Nitrogen.
LNT: Liquid Nitrogen Temperature.
NEST: Network 4 Energy Sustainable Transition.
OH: Optics Hutch.
ORR: Oxygen Reduction Reaction.
OTS: Ovonic Threshold Switch.
Pc: Phthalocyanine
PCM: Phase Change Memory.
PEC: Photo Electro Chemical.
PGM: Platinum Group Metal.
PIN: P-doped, Intrinsic, N-doped.
PMT: Photo Multiplier Tube.
PNRR: Piano Nazionale di Ripresa e Resilienza.
POLYX: Polycapillary X-ray optics.
PPR: Preordered Precursor Reduction
Q-XAS: Quick X-ray Absorption Spectroscopy.
REE: Rare Earth Element.
ReflEXAFS: Reflection Extended X-ray Absorption Fine Structure.
RHE: Reversible Hydrogen Electrode.
SDD: Silicon Drift Detector.
TEY: Total Electron Yield.
UGA: Université Grenoble Alpes.
WS: Water Splitting.
XAFS: X-ray Absorption Fine Structure.
XANES: X-ray Absorption Near Edge Structure.
XAS: X-ray Absorption Spectroscopy.
XEOL: X-ray Excited Optical Luminescence.
XES: X-ray Emission Spectroscopy
XRD; X-ray diffraction.
XRF: X-ray Fluorescence.

1. Introduction

The LISA beamline is the Italian CRG beamline at the European Synchrotron Radiation Facility ESRF. It is the continuation of the previous GILDA project that has been active from 1994 to 2014, though with some differences. First, LISA has a completely different X-ray optics based on beam focusing with a toroidal mirror rather than a sagittal focusing crystal. Secondly, the scientific case has been changed from GILDA by discontinuing the X-ray diffraction activity to focus more deeply on X-ray Absorption Spectroscopy (XAS). From a financial perspective, LISA is fully funded and managed by the Consiglio Nazionale delle Ricerche (CNR) via the IOM institute whereas a strong partnership with the CERIC ERIC has been recently signed.

LISA is fully dedicated to XAS that can be carried out in conventional 'transmission' and 'fluorescence' modes as well as using more 'material targeted' data collection techniques like Grazing Incidence or Total Reflection XAS, Total Electron Yield, X-ray Excited Optical Luminescence or surface mapping. Data are collected by scanning the energy in stepping mode but recently the continuous scan mode has been tested with some success.

The period 2020-2024 has represented a hard challenge for LISA with the coincidence of two major events: the start of the EBS storage ring and the Covid-19 pandemic. The beamline with its new instrumentation was completed at the end of year 2018 and recommissioned on the EBS beam in year 2020 after the confinement period. The most relevant aspect of the new source has been a shrinking of the beam from the previous 200×200 μm to slightly below 100×100 μm due to the smaller source size. This has led to an increase of the available beam intensity in all the applications needing a small source like grazing incidence experiments. The new machine refilling scheme, with the top-up mode hourly refilled, had an impact on some experiments, needing the synchronization of the data collection with the machine refilling to avoid spectral distortions linked to the related electron beam movements.

The scientific activity has strongly shifted towards green chemistry with a considerable part of the experiments dedicated to (photo)electrochemistry. The availability of an ESRF support laboratory for electrochemistry has considerably facilitated the adoption of this new topic at the beamline. Materials science is also very active at LISA with research on materials for electronics and magnetic materials. Another field that has recently found a renewed interest has been the cultural heritage with the research on degraded pigment boosted by the adoption of the joint Fluorescence - Total Electron Yield data collection mode that permits the analysis at the same time on the surface and in the bulk of the sample. On the other hand, other activities like biophysics and earth science have had a less prominent role.

2. Description of the technical configuration of the beamline

Overview

LISA takes the beam from a single bend source located at about 26 m from the main slits. The total fan collected is about 0.6 mrad hor and 60 μrad vert. The overall scheme of the beamline is shown in Figure 1 [Daca-19]

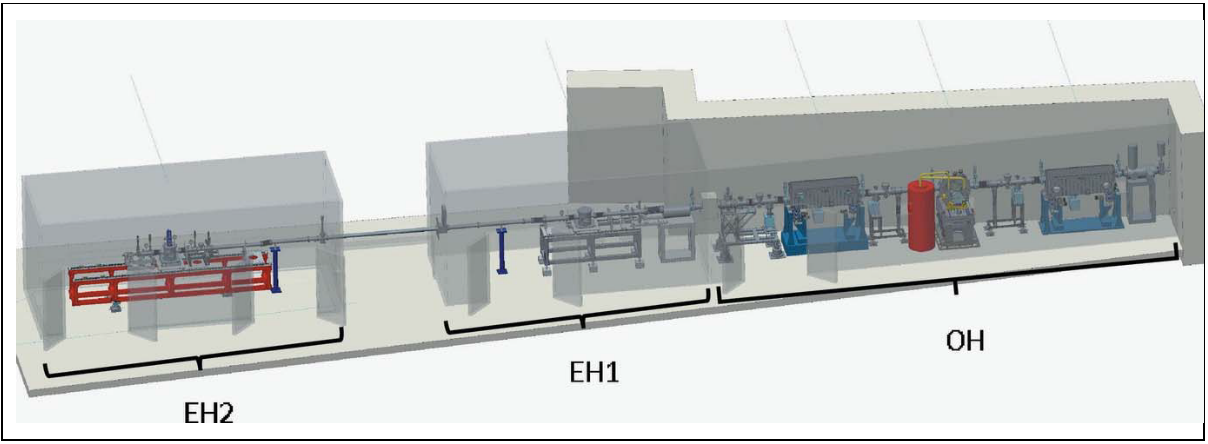

Figure 1: Layout of the LISA-BM8 beamline [Daca-19].

The optical scheme is composed of a first cylindrical collimating mirror, a double crystal fixed-exit monochromator and a second focusing toroidal mirror as shown in Figure 2 [Daca-19]:

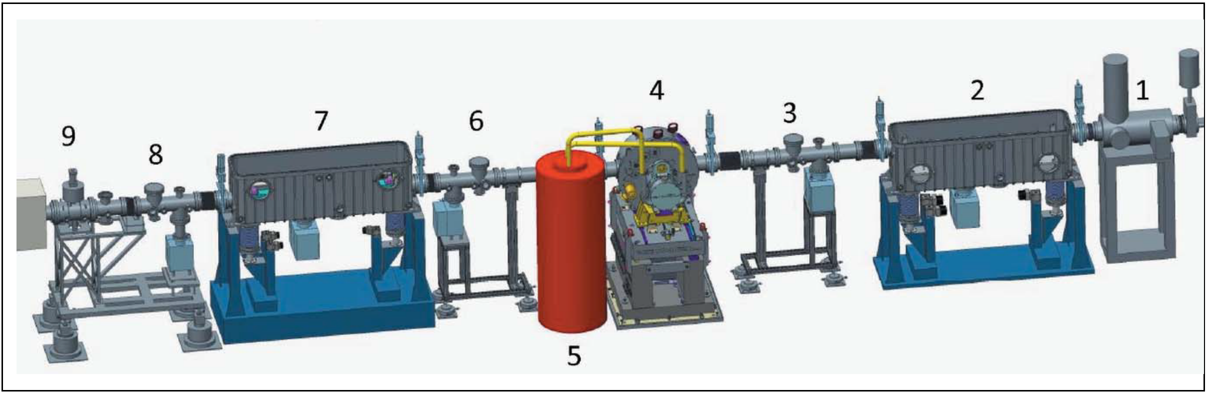

Figure 2: Layout of the optic hutch of LISA with the optical elements. 1=principal slits, 2: firs collimating mirror, 3: beam monitor, 4: monochromator, 5: cryo-circulator, 6, beam monitor, 7: second focusing mirror, 8: beam monitor, 9 beam shutter [Daca-19].

The mirrors have a double coating Si and Pt and have a fixed incidence angle at 2 mrad. This value ensures an operational energy range for the Si coating up to 15 keV above the Pt-L edges (11.5-13.8 keV). The Pt coating is then used above 15 keV, thus avoiding the associated strong discontinuities, and up to 40 keV. For higher energies the mirrors are removed from the beam path and the beamline lowered to match the new beam height. The first mirror is cylindrical and collimates the beam in the vertical plane in order to maximize the energy resolution of the monochromator and to avoid dependence on the vertical slit aperture. The second mirror is toroidal (placed at 34 m from the source) focuses at 17 m from its center in the middle of the EH2 hutch. The focal configuration for the horizontal plane is then 2:1 and it ensures a beam size of about 100×100 μm on the focal spot.

The monochromator is equipped with two crystal pairs: Si(111) and Si(311) with the first set operating in the range 5-30 keV at high luminosity and the second in the range 5-70 keV operating at high resolution/energy. Using the Si(333) reflection the energy range can be extended to 90 keV. The low-energy limit of the Si(111) crystal is not due to Bragg angle limitations but to the presence of a thick (0.5 mm) Be window in the Front End that cuts severely the beam below 5 keV. The crystals are cooled with Liquid Nitrogen in order to work in the temperature region of minimal thermal expansion of Si and to limit energy shifts due to thermal load. The flux is in the 10^{11} ph/s with the Si(111) crystal and in the 10^{10} ph/s with the Si(311) crystal. The measured energy resolution is in line with the theoretical calculations.

Experimental hutches

LISA has two experimental hutches, the first one EH1 is located a few meters downstream the optics hutch. EH1 has a wide unfocused beam (about 1×2 mm^2) and it is used for experiments in transmission mode with inhomogeneous samples. The second hutch EH2, located a few meters downstream EH1, has a focused beam (about 100×100 μm^2) and is dedicated to experiments that require a small beam, like XAS in fluorescence mode, Grazing Incidence X-ray Absorption Spectroscopy (GIXAS), reflectivity EXAFS (ReflEXAFS), or experiments with diluted or very small samples. The experimental apparatuses (vacuum chambers, ion chambers, detectors) are installed on the EH2 bench, and can be shifted along the beam path, via sliding plates in order to accommodate additional instrumentation, and to adapt to the user's needs.

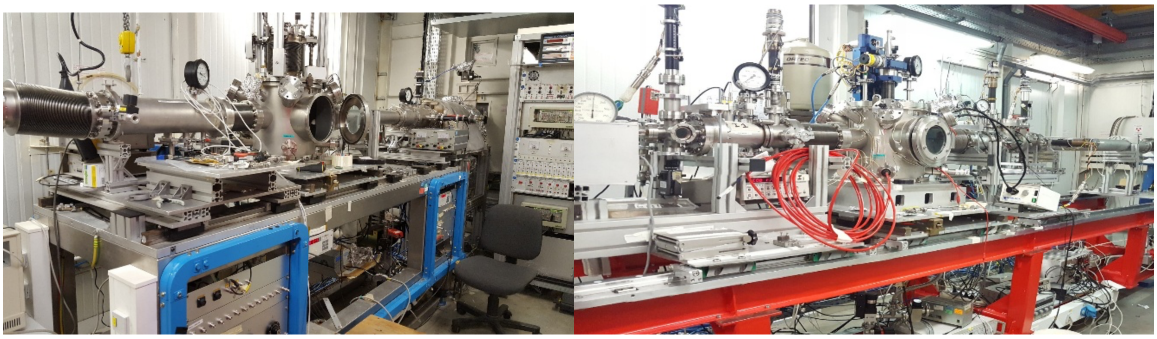

Figure 3: Left: first experimental hutch EH1. Right: second experimental hutch EH2.

Sample environment

Both hutches are equipped with vacuum chambers and cold finger manipulators which can be easily exchanged. The first one, usually located in EH1, has been custom-made by Trento University and can operate between 80 K and 500 K with a LN_2 flow. The second one, located in EH2, has been manufactured by Oxford Instruments (Microstat-He) and can operate between 20 K and 450 K using a He/LN_2 flow. A third manipulator is also present and is used with bulky/heavy user cells. The manipulators can be installed on any vacuum chamber in the EHs. It is also possible to use the compact furnace developed by ESRF (Microtomo) that allows measurements at high temperature (up to 1000 K), under a controlled atmosphere, suitable for in-situ and in operando experiments.

For pump and probe experiments a pulsed laser operable at the full rate of the 16b beam (5.6 MHz) is available. The laser has a wavelength of 400 nm, a pulse duration 100ps-1ns and pulse energy of 100 pJ. The beam can be sent to the sample via an optical fiber and a focusing lens. A suitable electronic module (BCDU8, developed by ESRF) allows the synchronization between the X-ray flashes and the laser whereas a fast photomultiplier can be used for checking the delay between the laser and X-ray pulses.

Regarding electrochemistry experiments, the users provide their own cell to be used on the beamline. This revealed to be preferable to the development of cell provided by the beamline as each user can conduct the experiment with a well-known and characterized cell.

Nonetheless, LISA provides a potentiostat from the ESRF electrochemical lab to carry out the sample treatment.

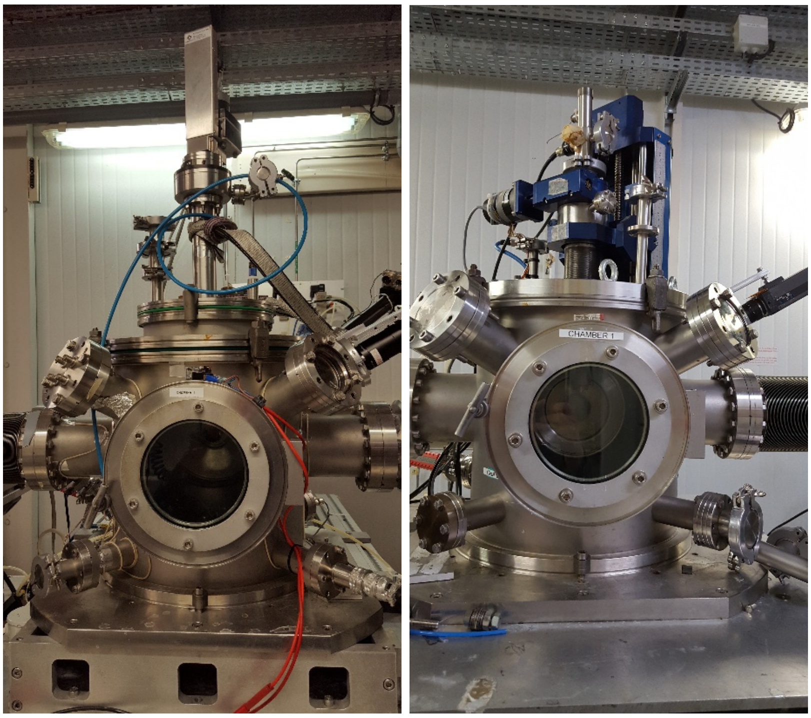

Figure 4: Experimental chamber with mounted the Trento manipulator (left) and the Oxford manipulator (right).

Detectors

Ion chambers

LISA has five ionization chambers (ICs): two located in EH1 and three in EH2. Depending on the energy of the X ray beam, different gases are used to fill the chambers to achieve an optimal absorption: N_2 for the energy range 4 - 15 keV; Ar for 15 - 35 keV; Kr above 35 keV. The ICs are read by picoammeters (different Keithley models) followed by Voltage-to-frequency converters in order to minimize the electronic noise.

Fluorescence

For measurements in fluorescence mode two High-Purity Germanium (HPGe) detector arrays are available. They are both manufactured by Ortec, the first with 12 elements (normally in use), the second with 13 elements used as spare. In both cases the readout is made by digital analysis of the output pulses using the XIA-DXP system. A 4-element Silicon Drift Detector (SDD), ARDESIA, developed in collaboration with Politecnico di Milano [Hafi-19] is also available. This detector is particularly effective for fluorescence experiments at E < 20 keV, offering high count rates (up to 1Mcps/channel) and good energy resolution (down to 150 eV FWHM @ 6.4 keV). The instrument has been realized to fit inside the sample chamber with a finger-like structure and allows operation in vacuum. It can be moved closer or farther from the sample via a motorized platform. The readout is made by using the commercial XIA-DXP system. Several Silicon PIN photodiodes used in photovoltaic mode are also available when the energy resolution is not needed in fluorescence measurements.

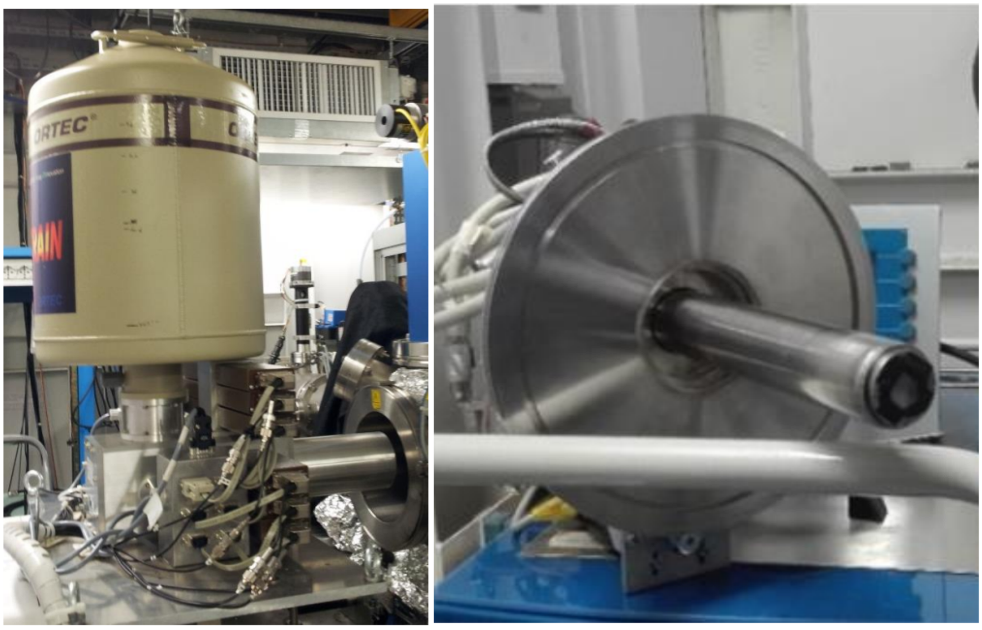

Figure 5: Left: the 12-elements HP-Ge detector; Right: the 4 elements SDD with the vacuum flange.

Total Electron Yield

A state-of-the-art apparatus for Total Electron Yield (TEY) has been developed in collaboration with the Institute of Materials Science Leibniz University Hannover. It consists of a base and a cover plate, which acts as the anode, both made of aluminum, held together by four insulating spacers. The TEY (Auger and secondary electrons) is collected by the anode kept at a moderate voltage (≈ +45 V). The resulting current is converted to a voltage signal via a Keithley amplifier. The base can host up to 10 specimens mounted on round plates which are clamped to the metallic frame, ensuring an improved electrical contact of the sample to the ground. The cover plate has 10 holes aligned to the samples, to allow the transmission of the X-ray beam. It is possible to use spacers of different lengths to adjust the distance from the anode to the sample and accommodate samples of various sizes. The holder can work either in vacuum or in a He atmosphere (usually 200 mbar) acting as an electron multiplier. Moreover, the holder allows to measure TEY and fluorescence simultaneously by adjusting the incidence angle of the X-ray beam and allowing to obtain simultaneously ‘bulk’ and ‘surface’ spectra.

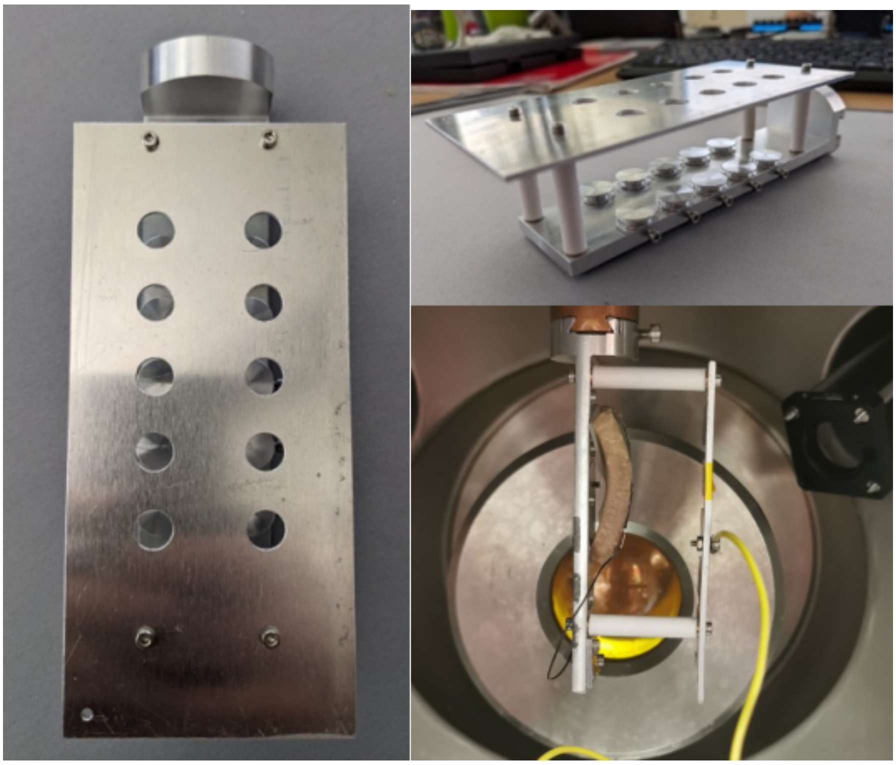

Figure 6: Left: top view of the TEY holder. Right: side view of the holder empty and with a sample mounted inside the experimental chamber.

X-ray excited optical luminescence (XEOL)

A system for the collection of XAS-XEOL data is also available: it consists of a lens (BK7 glass) collecting the emission from the sample coupled to a silica optical fiber. The system is mounted inside the measurement chamber and can operate in vacuum and with the sample at Liquid Nitrogen Temperature (LNT). The fiber runs out of the chamber via a feedthrough and it illuminates a fast photomultiplier tube (PMT, model HAMAMATSU H3164-10) sensitive in the range 300-650 nm. Band-pass optical filters (bandwidth 10 nm) can be mounted between the tip of the fiber and the PMT in order to select the desired optical emission band in the visible range. When working in 16b or 4b mode the PMT pulses can be windowed by a fast gate (Philips mod 744) synchronized with the X-ray flashes, thus realizing a time-resolved data collection.

Support laboratories

The laboratory associated with the beamline is equipped with a wide range of instruments useful for sample handling and preparation in view of experimental measurements. Standard equipment includes fume hoods for safe handling of volatile chemicals, analytical scale for precise weighing of reactants, mortars and agate pestles for mixing and homogenization of samples and binding materials (cellulose, graphite and boron nitride available) as well as dies of different diameters (5, 13 mm) used in conjunction with a press for the preparation of pellets for solid samples. A glove box filled with Nitrogen is available for handling air sensitive materials whereas a desiccator system (paired with a membrane pump) and an oven can be used for drying samples. A muffle can also be used for temperature-controlled treatment of samples in air up to 900°C. Filtration and deposition of samples from liquid solutions can be made with filters of different pore sizes. The beamline is also equipped with spatulas, syringes, Pasteur and Gilson pipettes as well as glassware for mixing, titration and reaction of samples alongside a hotplate with magnetic stirrer. The laboratory is equipped with chemical storage cabinets and a fridge/freezer for safe storage of reactants and solvents. The laboratory follows a strict safety protocol and features personal protective equipment available to users (gloves, lab coats, goggles and masks) and is designed to support the preparation of solid, liquid, and powder samples required for beamline experiments.

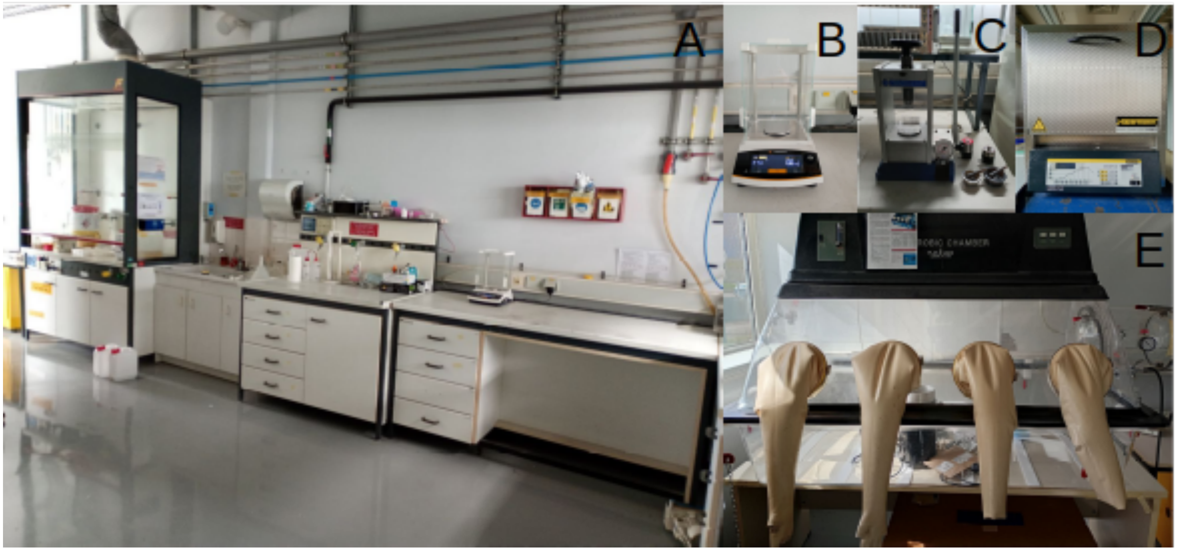

Figure 7: Laboratory for sample preparation (A), analytical scale (B), press with dies and mortars (C), furnace (D) and glove box (E).

Data processing and analysis software

During this period the beamline has remained with the SPEC control environment. Nonetheless, we have implemented the standard data management scheme of ESRF that complies with the FAIR principles. All data collected after 2022 now have a Digital Object Identifier (DOI) and can be retrieved from the ESRF data portal by the users' team and will be open to the public after the embargo period. The data collected at LISA are pre-processed with software tools developed in house (see Table 1). All the tools developed at the beamline are written in Python to be easily further developed and shared. The main directions of software developments by the staff can be summarized in two categories: new data collection and data conversion. The first was to make use of the existing SPEC routines to collect more data more easily and add flexibility to beamline experiments. This led to the creation of a new mapping acquisition tool and a full X-Ray Fluorescence (XRF) spectra XAS acquisition tool. With the mapping acquisition tool, it is possible to acquire XRF maps at different (fixed) energies. With the full XRF spectra XAS acquisition tool, it is possible to collect XAS spectra in fluorescence mode while storing the full spectrum at each energy point, giving more flexibility for data analysis later. Concerning data conversion, new tools have been developed to compel with the guidelines for data fairness and usability, following the international standards. Thus, XAS data are now converted into 'xdi' format while maps are converted into NeXus format.

Table 1: List of the codes developed at LISA for data pre-processing.

Software	**Deliverables**

Data conversion	• **Process data**: convert the data from ‘dat’ into the ‘xdi’ standard, inserting metadata useful for data analysis (e.g. crystal employed, d-spacing, current of the ring…) • **Correct data:** apply a final energy correction using the encoder of the monochromator.
Mapping	• **Raw data**: launches the data collection. The user selects the four corners of the region to map, the number of horizontal and vertical steps, the energy(ies) of irradiation, and the dwell time for each spot. The software launches the spec commands and collects the ‘edf’ spectra for each spot and one ‘dat’ file containing all the motor positions and the counters. • **Process data**: the ‘edf’ and ‘dat’ files are merged into a single NeXus file. • **Extracted data**: a second tool allows for summing spectra from different detector elements, normalizes them to the incoming flux, and applies dead time correction. The maps are extracted by selecting a ROI from the XRF spectra. Finally, data collected over the same spatial region at different energies can be subtracted or normalized, to highlight differences in the signal intensity of various chemical species of the same element. Such maps can then be saved.
XAFS with Full XRF spectra collection	• **Raw Data:** Allows for saving the full XRF spectra generated at each energy step of an XAFS analysis. The XRF spectra are saved as ‘edf’ file (one for each detector element), and a ‘dat’ file contains the other counters (Ionization Chambers, Monochromator encoder…) • **Process Data**: a second tool merges the ‘edf’ and ‘dat’ files into a single NeXus file.

As a contribution to open science, it is worth noting the creation of the “LISA XAS Database” [Puri-24]. The database is openly available (https://lisa.iom.cnr.it/xasdb), and it contains XAS spectra of model compounds collected ad LISA.

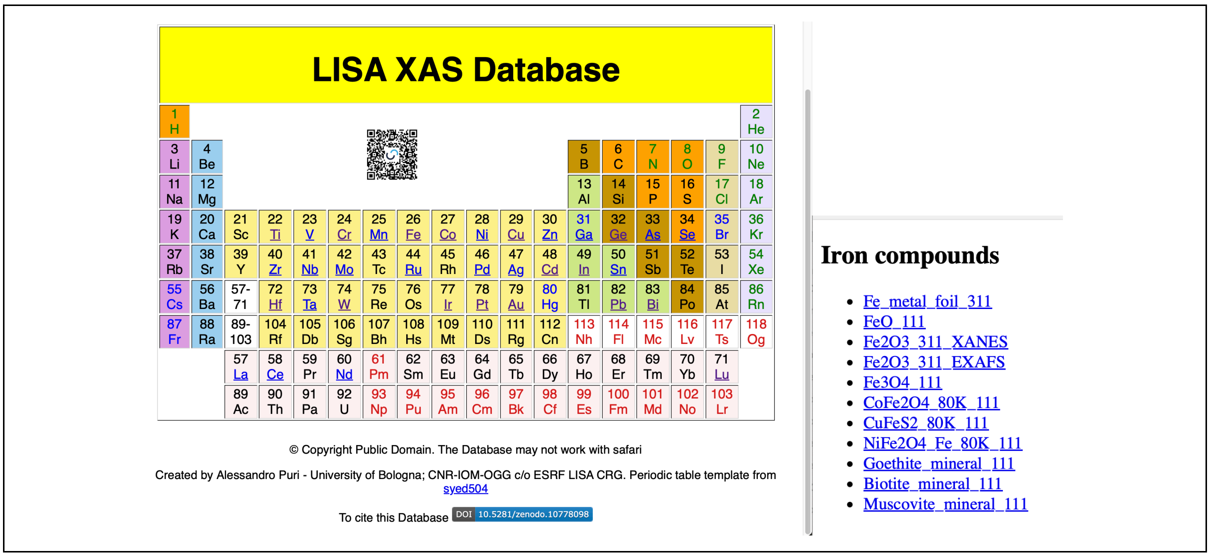

LISA XAS Database

1 H																	2 He
3 Li	4 Be											5 B	6 C	7 N	8 O	9 F	10 Ne
11 Na	12 Mg											13 Al	14 Si	15 P	16 S	17 Cl	18 Ar
19 K	20 Ca	21 Sc	22 Ti	23 V	24 Cr	25 Mn	26 Fe	27 Co	28 Ni	29 Cu	30 Zn	31 Ga	32 Ge	33 As	34 Se	35 Br	36 Kr
37 Rb	38 Sr	39 Y	40 Zr	41 Nb	42 Mo	43 Tc	44 Ru	45 Rh	46 Pd	47 Ag	48 Cd	49 In	50 Sn	51 Sb	52 Te	53 I	54 Xe
55 Cs	56 Ba	57- 71	72 Hf	73 Ta	74 W	75 Re	76 Os	77 Ir	78 Pt	79 Au	80 Hg	81 Tl	82 Pb	83 Bi	84 Po	85 At	86 Rn
87 Fr	88 Ra	89- 103	104 Rf	105 Db	106 Sg	107 Bh	108 Hs	109 Mt	110 Ds	111 Rg	112 Cn	113 Nh	114 Fl	115 Mc	116 Lv	117 Ts	118 Og
		57 La	58 Ce	59 Pr	60 Nd	61 Pm	62 Sm	63 Eu	64 Gd	65 Tb	66 Dy	67 Ho	68 Er	69 Tm	70 Yb	71 Lu	
		89 Ac	90 Th	91 Pa	92 U	93 Np	94 Pu	95 Am	96 Cm	97 Bk	98 Cf	99 Es	100 Fm	101 Md	102 No	103 Lr	

© Copyright Public Domain. The Database may not work with safari

Created by Alessandro Puri - University of Bologna; CNR-IOM-OGG c/o ESRF LISA CRG. Periodic table template from syed504

To cite this Database DOI 10.5281/zenodo.10778098

Iron compounds

- Fe_metal_foil_311
- FeO_111
- Fe2O3_311_XANES
- Fe2O3_311_EXAFS
- Fe3O4_111
- CoFe2O4_80K_111
- CuFeS2_80K_111
- NiFe2O4_Fe_80K_111
- Goethite_mineral_111
- Biotite_mineral_111
- Muscovite_mineral_111

Figure 8: Picture of the LISA database of XAS spectra of model compounds. For each element a clickable link leads to a list of available compounds. At present about 100 model compounds are included.

The database contains spectra in the ".xdi" format (the format presently recommended by the International XAFS Society) and it can be exploited by users for their data analysis or by students to get spectra for training. It is managed by Dr Alessandro Puri and it is continuously updated, also thanks to the contribution of users who agree to share the data on model compounds collected during experiments.

References

[Daca-19] d'Acapito, F., Lepore, G. O., Puri, A., Laloni, A., La Manna, F., Dettona, E., De Luisa, A. & Martin, A. (2019). The LISA beamline at ESRF. J. Synchrotron Rad. 26, 551-558. https://doi.org/10.1107/S160057751801843X

[Hafi-19] Hafizh I., Bellotti G., Carminati M., Utica G., Gugiatti M., Balerna A., Tullio V., Lepore G.O., Borghi G., Ficorella F., Picciotto A., Zorzi N., Capsoni A., Coelli S., Bombelli L., Fiorini C. - Characterization of ARDESIA: A 4-channel SDD X-ray spectrometer for synchrotron measurements at high count rates Journal of Instrumentation 14, P06027-1-06027-14 (2019). https://doi.org/10.1088/1748-0221/14/06/P06027

[Puri-24] Puri, A. LISA XAS Database, Zenodo, https://doi.org/10.5281/zenodo.10778098

3. Facts and figures

Comprehensive list of the beamline staff

The resident staff (scientists and technicians) at LISA have varied considerably in the years of the contract and the details are given in Figure 9.

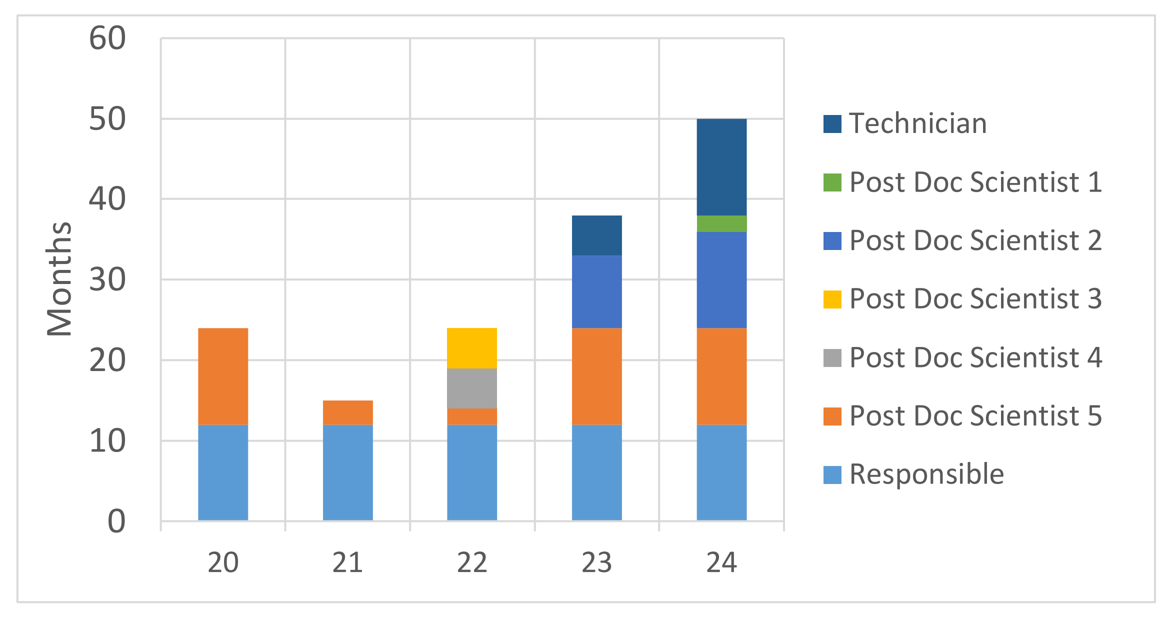

Figure 9: Staff of LISA in the years of the contract with the operative months.

The level of staff recommended by the contract is 36 months/y and from Figure 9 it is evident that this level has been reached only in 2023 and 2024 whereas in the previous years, LISA has been significantly understaffed. The agreements with Italian universities and with the CERIC-ERIC have enabled a considerable increase in staff over the past two years.

The staff have been active also in training with a series of students and visitors, who have spent a period of at least one month at LISA:

Table 2: Number of students (master & doctorate) having spent at least 1 month at LISA.

Year	Students
2020	1
2021	3
2022	4
2023	5
2024	1

In addition, LISA is active in the training of young scientists through the following programs:

- HERCULES school. LISA regularly holds lectures on the XAS technique for the participants.

- Users Meeting. LISA regularly holds practicals on the XAS technique for the participants.
- Université Grenoble Alpes (UGA). LISA has held 2 training days (2022 and 2024) for the Master 2 students of the “Quantum matter” course at UGA.

Statistical analysis about the use of the beamline:

The beamtime available at LISA is divided into different programs:

- Public beamtime
- CRG beamtime
- IHR
- BLC

The public beamtime is managed by the ESRF review committee, whereas part of the CRG beamtime is managed by the CERIC-ERIC via a specific agreement. The remainder is allocated to In House Research (IHR), through which the staff can carry out their own research in collaboration with external projects, or Beam Line Commissioning (BLC). The user’s mode program is dominated by activities on materials science MA (materials for electronics, high entropy alloys), chemistry CH (batteries, fuel cells and electrolyzers) and hard Condensed matter structures (HC) as shown in Figure 10.

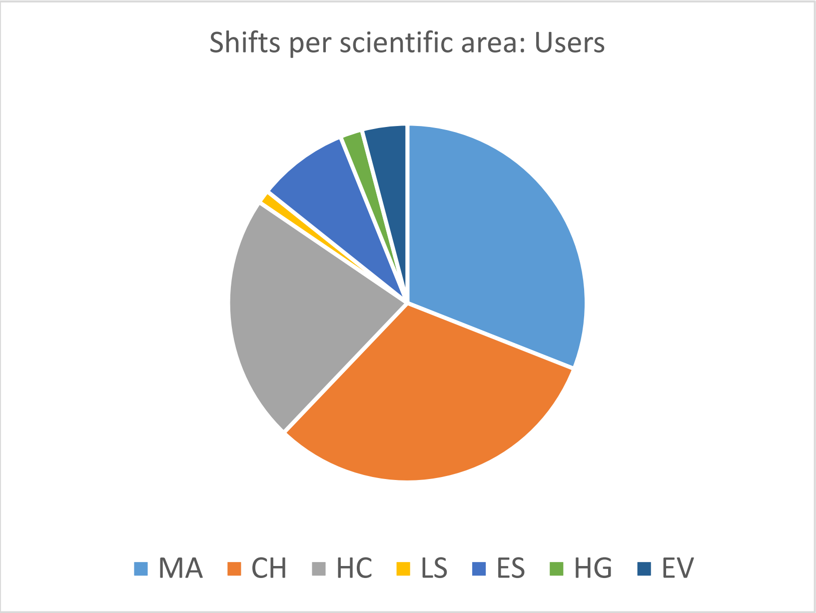

Figure 10: Delivered shifts per scientific area in the period 2020-2024. Merge of ESRF and CERIC experiments. MA= Applied Materials Science, CH=Chemistry, HC=Hard Condensed Matter Science, LS=Life Science, HG=Cultural Heritage, EV=environment.

A different situation is revealed when considering the scientific areas covered by the In-House Research program (Figure 11).

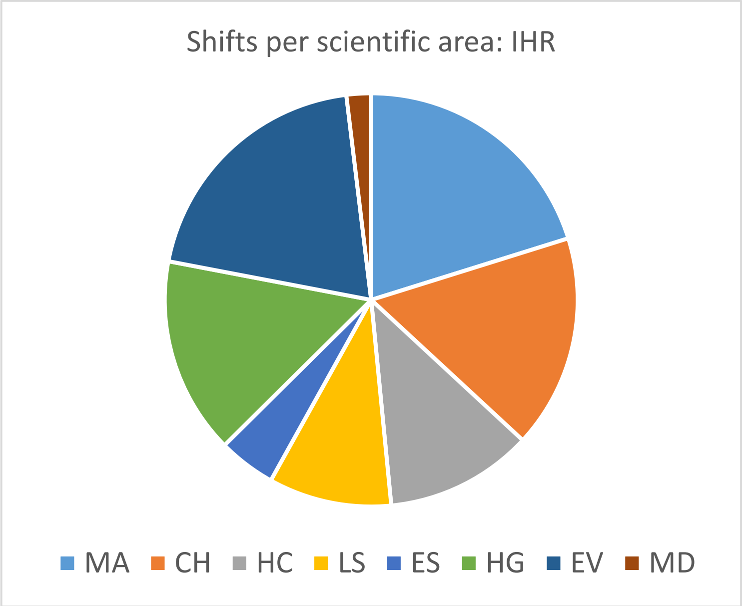

Figure 11: Delivered shifts per scientific area in the In-House Research (IHR) program. The codes for the scientific topics are explicated in Figure 10.

In this case the topics of Cultural Heritage (HG) and environment (ES) take a more prominent role, reflecting the activity of the postdocs and students. A considerable part of the activities has been focused on the development / consolidation of new techniques like TEY or mapping for cultural heritage and chemistry.

Regarding the nationality of the users (Figure 12), the Italian scientific community largely dominates the access to LISA, followed by Poland, France and Germany. The Polish and Greek communities have grown significantly after the launch of the CERIC user program.

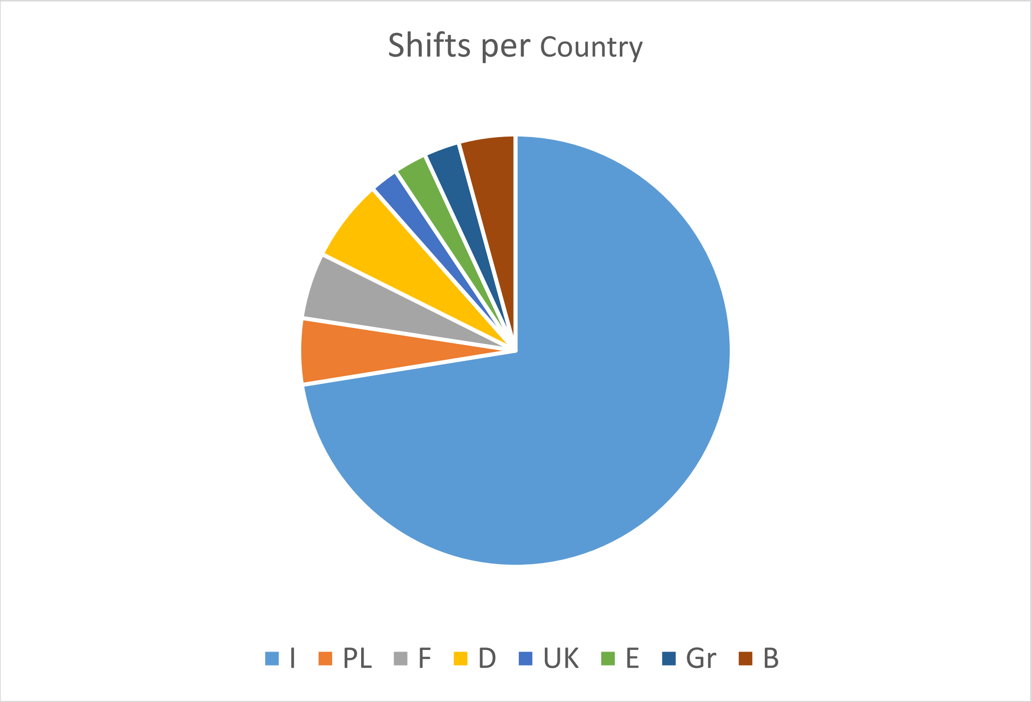

Figure 12: Delivered shifts per country of the main proposer in the period 2020-2024. Merge of ESRF and CERIC experiments.

The main activities of BLC have been the usual maintenance of the beamline and, during certain periods in years 2021 and 2023, dedicated to the recovery from major material failures.

Figure 13 illustrates how the total shifts are distributed across categories.

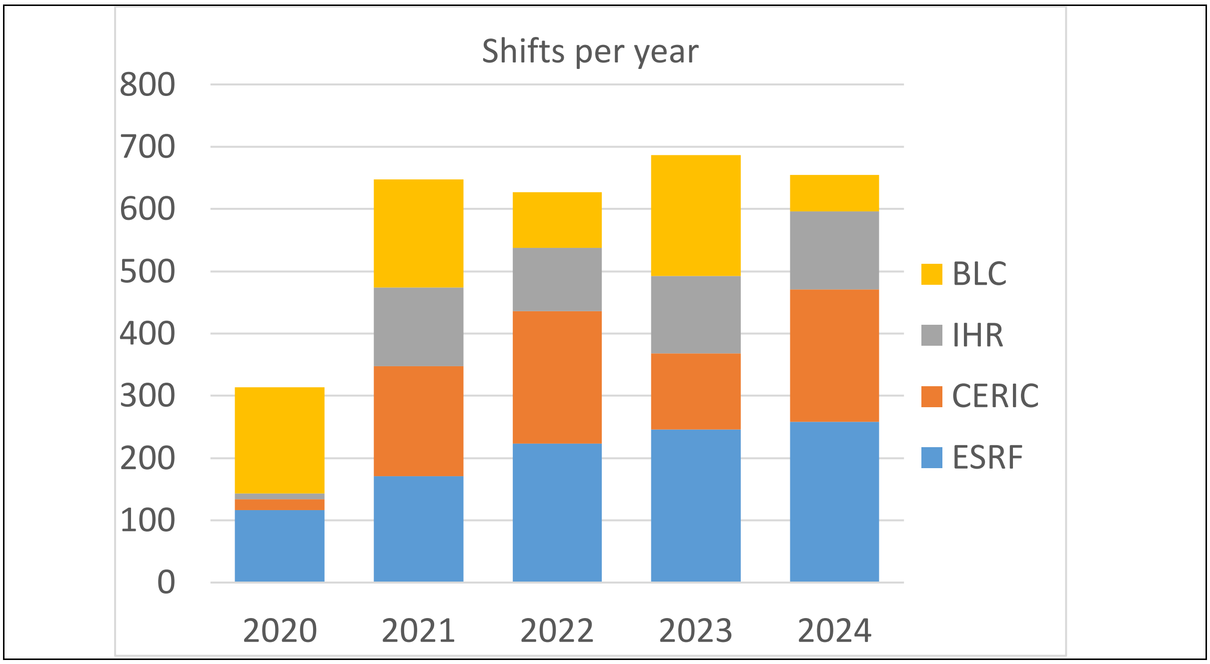

Figure 13: Shifts per year delivered by LISA divided in the four categories 'BLC', 'IHR', 'CERIC', 'ESRF'.

LISA is a beamline highly requested by users as shown in Figure 14.

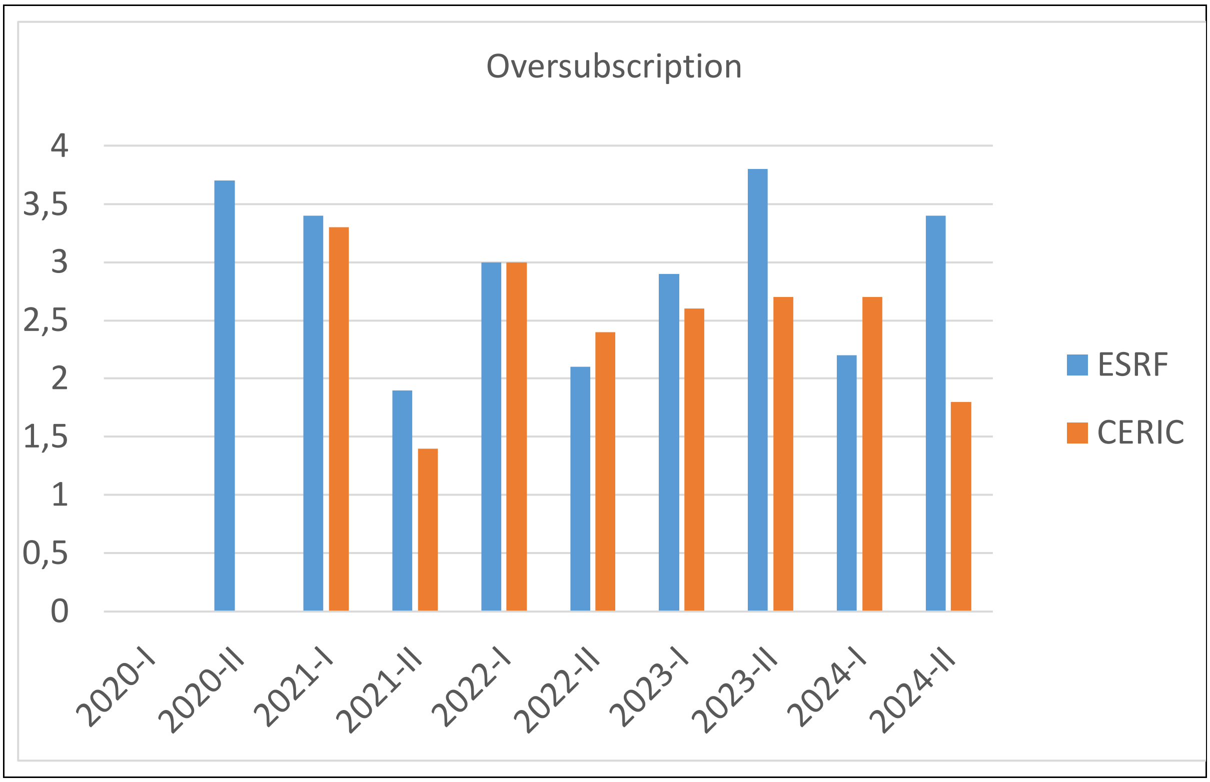

Figure 14: Oversubscription on the User quotas ESRF and CERIC.

The average overbooking in the period of observation is 2.9 on the ESRF quota and 2.5 on CERIC, indicating strong appreciation from the community.

4. Science programmes

LISA is active in several science programmes. Most of them heavily involve the beamline staff either as XAS experts for the development of appropriate data-collection, data-analysis methods or for their scientific background in selected topics.

Materials science

A considerable part of the LISA activity regards the broad topic of materials science. In this case, some peculiar experimental techniques focused on surface analysis (Grazing Incidence XAS and Total Electron Yield) have represented a precious tool for the study of some classes of samples. The availability of the XEOL instrumentation has also enabled the realization of advanced studies on luminescent materials. The LISA team has been deeply involved in studies involving these advanced analysis techniques.

High-Entropy Alloys

User driven projects

A first topic of considerable relevance in the activity of LISA is the research on High Entropy Alloys (HEAs) [20-Fant, 22-Fant, 23-Joub, 24-Fant1, 24-Fant]. These are intermetallic alloys that exhibit several interesting properties for different applications namely medicine (high biocompatibility, hardness) or energy (magnetocaloric effect). Typically, these alloys possess an overall well-defined crystal structure (cubic, either face centered fcc or body centered bcc) but the crystallographic sites are randomly occupied by the different components of the alloy. The main basic scientific problem in the case of metallic HEAs is how truly ‘random’ the material is, i.e. whether there is a possible chemical ordering (i.e. a preferential coupling between given elements) and its possible relationship with the physical properties of the alloy. The samples are usually obtained in ribbons that cannot be thinned, in general, to the appropriate dimensions for XAS experiments in transmission mode. In this case, the use of the Total Electron Yield emission from the sample and the comparison with the standard Fluorescence Yield proves fundamental as it permits to work with thick and concentrated samples. This activity has been the result of the collaboration of a group in Berlin (Technical University of Berlin) and the beamline staff, and it has developed through several experiments in the last five years. The random nature of the material was found manifests as an alteration of the number of neighbours or bond distances. Figure 15 shows the correlation between local distances and Vickers Hardness in a series of Ni-based HEAs [24-fant]. These studies will help the groups to develop effective methods to produce random HEAs with the desired properties.

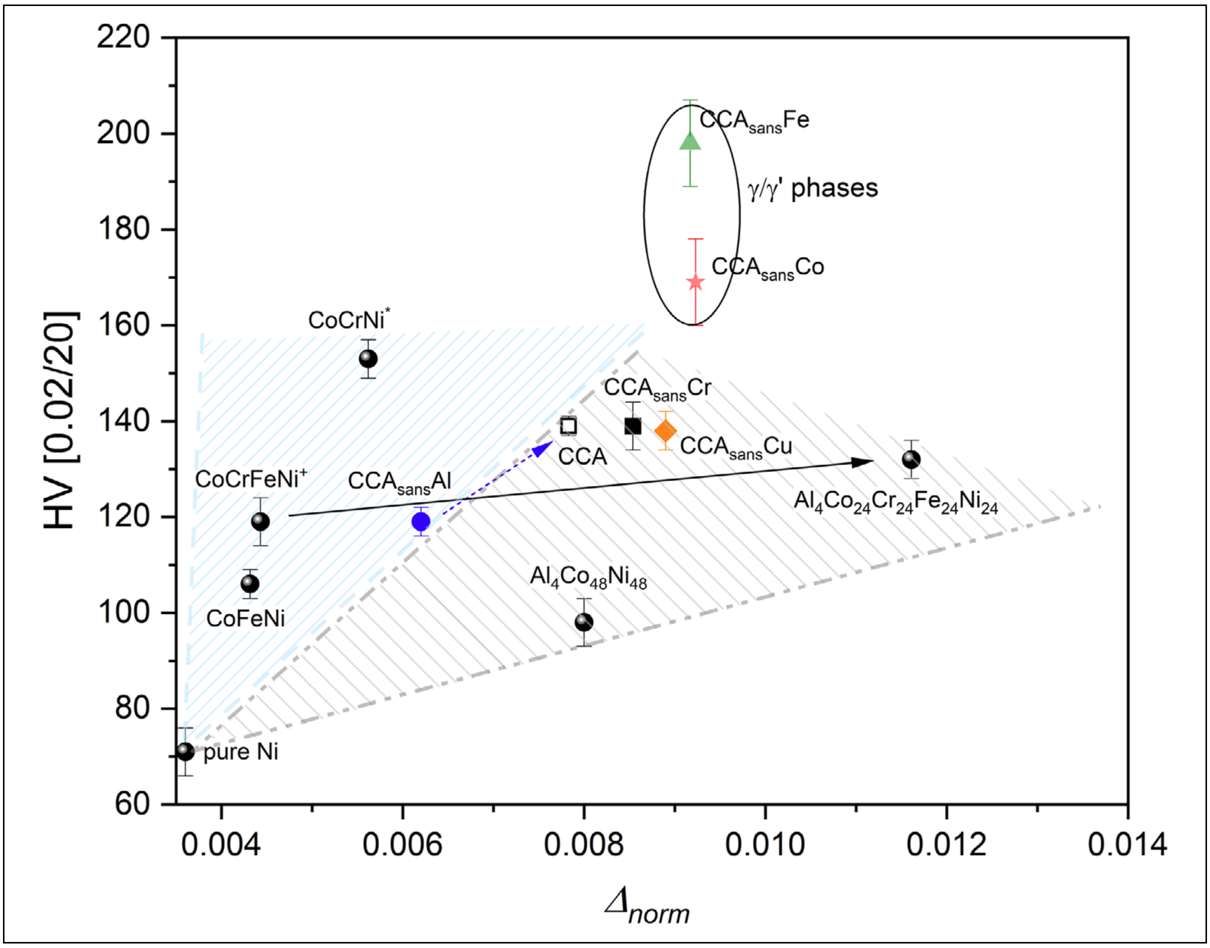

Figure 15: Dependence of Vickers Hardness (VH) in different Ni-based HEAs on the parameter Δ_{nor}. This parameter (see definition in 24-fant]) is calculated from the difference of bond lengths seen by XAS (so including local effects) with those seen by XRD (only long-range view) so reflecting the chemical ordering of the alloy. Figure from [24-fant].

Materials for electronics

Collaboration between users and staff

Materials for electronics have been the subject of many experiments at LISA, originating from the collaboration of the staff with the nearby CEA-LETI laboratory. One of the main problems at present, in order to produce devices with high performances and low energy consumption, is the realization of computer memories that do not need continuous power supply and that can store a large quantity of data. At this purpose, phase change materials constitute an interesting solution although presenting problems of long-term retention. In the studies presented here, phase-change materials have been investigated with the aim of relating the local structure to the physical properties of the materials like resistivity or memory state retention over time. These materials are grown following the procedures typical of those of microelectronics, so they consist of thin films with thicknesses ranging from tens to hundreds of nanometers. For this, the capability of LISA to carry out data collection in grazing incidence mode has proven to be fundamental as it permits to minimize the unwanted signal from the substrate. The fact that the beam is focused permits to have its full intensity on the sample even in low-incidence angle conditions, thus enabling the collection of high-quality spectra. Phase change materials are a class of materials that constitute part of the scientific activity of the beamline responsible (F. d'Acapito) and several papers treat this topic [20-Verd, 20-Daca, 20-Noe]. These studies have permitted to identify the structure of layered chalcogenide materials for interfacial Phase Change Memory [20-Daca]. In the field of Ovonic Threshold Switching (OTS) materials, it was possible to evidence the beneficial effect of Nitrogen doping of GeSbTe (GST) systems by preventing the formation of homopolar bonds [20-Verdy]. The support provided by EXAFS to the structures of GST materials obtained by ab–initio molecular dynamics have made possible to demonstrate the importance of collinear bonds in the onset of the OTS mechanism.

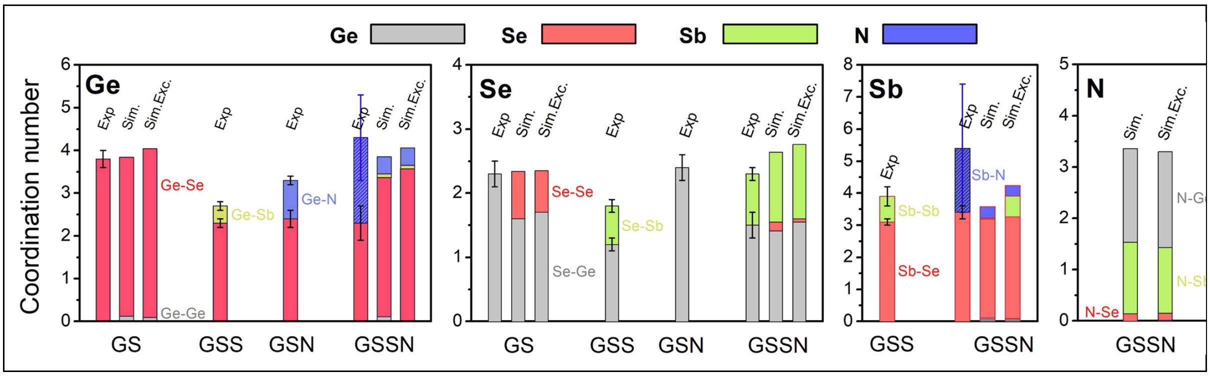

Figure 16: Comparison of coordination numbers obtained by EXAFS (Exp) and by structural simulation confirming the validity of the theoretical models In GeTeSbN materials. This validation of the ab-initio structures has permitted to interpret further details of the theoretical models out of which the formation of the bond alignment explaining the OTS effect.

The development of methods for the full ab-initio simulation of EXAFS spectra by the LISA staff [24-daca] has enabled in some cases to identify a structure among many proposed in literature. The use of Molecular Dynamics for the theoretical simulation of EXAFS spectra has therefore allowed the identification of the structure of layered GST materials for iPCRAMs [20-daca] and it has also been demonstrated to be effective on 2-dimensional materials like WSe_2 [24-daca]. These studies provide atomistic models describing PCMs and iPCMs or linking electronic excitation to structural rearrangements in OTS materials, establishing a unifying mechanism that bridges phase-change and threshold switching behaviours, and enabling the design of more stable and CMOS-compatible memory devices

Luminescent materials

Collaboration between user and staff

The research of novel luminescent materials is extremely active at present and finding the relationship between structure and luminescent properties is fundamental for the optimization of the materials. This has a considerable social impact because, considered the wide use of displays in computer and smartphones, an improvement in this field would mean a reduced consumption of these devices. The problem with the materials studied here is their poor stability with time. The availability of peculiar methods for the XAS data collection on luminescent species (the X-ray Excited Optical Luminescence - XEOL instrument) at LISA is particularly appreciated by the community. With this apparatus, a number of studies [see notably 18-Gran] have been carried out as a longtime collaboration between the beamline staff (F. d'Acapito) and the KU-Leuwen (D. Grandjean and group) for the characterization of luminescent systems. In particular, small metal oligomers embedded in zeolites were studied as they present an extremely high quantum yield. The high luminescence exhibited by these materials have enabled an effective data collection in XEOL mode, which subsequently allowed a precise determination of the structure of the small metal clusters. The paper [24-Sun] was dedicated to a novel material for a photoluminescent oxygen-sensing probe based on Ag clusters in Faujasite. The use of XEOL at the Ag-K edge revealed the structure of the luminescent clusters as shown in Figure 17.

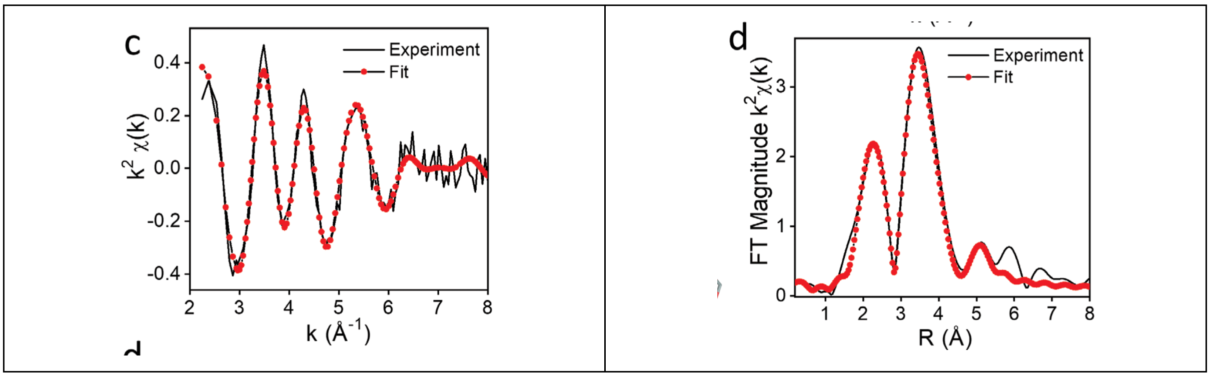

Figure 17: XAS-XEOL signal and related Fourier transform in the Ag- doped zeolite [Sun-24].

The analysis shown that the XEOL signal can be fitted with a mixture of Ag_4 and Ag_6 clusters. Further studies exploiting XEOL [romo-24] have permitted to evidence the structure of Ag oligomers in a matrix alternative to zeolites: titanosilicalite. From these results the groups aim to produce materials with a better time stability.

Other studies on optical materials conducted in the conventional data collection benefited from the capability of LISA to provide an intense beam and/or the opportunity to work in grazing incidence conditions for surface thin films. In the field of materials for photovoltaics, it has been possible to determine the incorporation site of Vanadium in In_2S_3 [23-ghor], a material for Intermediate Bands solar cells. The EXAFS analysis identified the site as the octahedral one and that permitted then to guide further theoretical studies on the band gap in this material. In another study on materials for photovoltaics, in this case nanoclusters of $Ag_xBi_{1-x}S$ [20-kesa], the comparison of experimental and ab-initio simulated EXAFS spectra facilitated the identification of the local structure around Ag as that of Matildite with a random Ag/Bi substitution.

Magnetic materials

User driven projects

In the field of magnetic materials, a number of experiments at LISA have been focused on methods to produce magnetically anisotropic alloys with the tetragonal $L1_0$ structure of the type Fe(Co)Pt or Fe(Co)-Pd to produce ferro- or para- magnetic materials. In this case the goal is to identify a method to obtain the alloys with the mildest conditions (namely, a lower temperature for the thermal treatment) so to reduce the resources needed for their production. A way explored by the group of S. Laureti (CNR-ISM Roma) has been to thermally treat appropriate salts that contain the alloy metals (Preordered Precursor Reduction, PPR) method to remove the original ligands and obtain the $L1_0$ structure at temperatures lower than those used in the conventional methods. The study shown in [23-laur] has benefited from the availability at the beamline of the quick-XAS data collection mode, that allowed the monitoring of the evolution over time of the salt while being heated in the reaction cell.

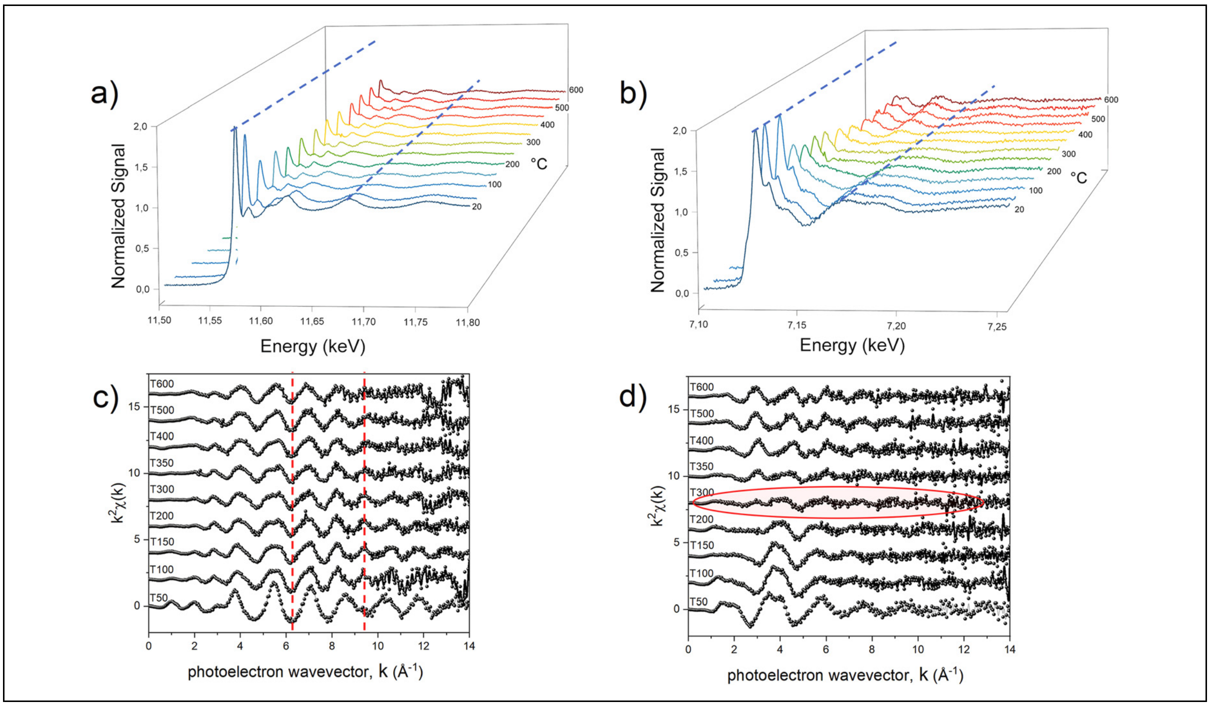

Figure 18: Pt-L_3(left) and Fe-K (right) spectra collected in the microtomo cell during the annealing of the precursor salt for the formation of the L1o FePt ordered alloy. Each spectrum was collected in 20s.

The study in [23-laur] allowed assessment of the efficiency of the PPR method to obtain the chemically ordered FePt alloy at lower temperatures than other methods. This finding was confirmed and extended to ternary compounds in a subsequent paper [24-capo] with an XAS study focusing this time on (Fe,Mn)Pt alloys. This has evidenced the effectiveness of the principle so opening the way for a possible use in industrial processes.

Electrochemistry

The beamline has been deeply involved in new research in the field of electrochemistry field, thanks to the possibility of performing ex-situ sample characterization and collecting in-situ and operando data. The latter is extremely important to study the evolution of the material along with the potential change applied during the ORR (Oxygen Reduction Reaction) and HER (Hydrogen Evolution Reaction) reactions, and the modification occurring with multiple cycles. Besides, the beamline has been involved in different water-splitting experiments. The set-up of the beamline and the size of the measurement chamber is one of the strengths of the electrochemistry experiments, as it allows for the development and installation of custom electrochemical cells, and to perform numerous different experiments in different geometries and with different illumination conditions [24-Deam, 20-Mala]. The use of an appropriate manipulator (Huber cradle and translator) also extends the possibility to perform operando GIXAS measurements [24-Berr].

New materials for Electrocatalysis

Collaboration *between* user and staff

Platinum Group Metals (PGMs) are widely used in the catalysis field for their high efficiency. Nonetheless they present remarkable drawbacks (high cost, scarcity and polluting extraction methods, stability of micro- and nanoparticles on carbon supports; and poisoning with CO) so 3d-metals are now being studied as alternatives for the creation of active sites for CO_2-

Reduction Reaction, ORR, and HER. The beamline has focused its activity to studying both the formation of these materials and their behaviour.

The study of the formation of active sites of Ni and Fe with Phthalocyanine (Pc) pyrolysis [24-Muhy, 24-Mirs] has been carried out at the beamline with an active collaboration of the local staff. The possibility of employing the microtomo furnace and operating with different atmospheres has been essential to studying the formation of the active Ni and Fe sites during the pyrolysis process, and their transformation after the exposition to air, allowing the discrimination of the byproducts and the correlation of the structure changes with the electrochemical performance. In both experiments, the samples were studied in situ during the pyrolysis (from room temperature up until 800°C) in a reducing atmosphere (HydroStar or Ar) and ex-situ, after cooling sample in air.

The study of the pre-peak intensities of the FePc has made it possible to observe how the dissolution of the Pc structure occurs until 500°C. The increase in temperature in the in-situ measurements shows the desorption of oxygen and the change from a pyramidal to a planar geometry. In parallel, the small changes in the pre-peaks of the ex-situ measurements suggest that after being exposed to air, oxygen is again adsorbed by the FePc with the formation of $(FePc)_2O$. Additionally, the Linear Combination Fitting (LCF) was employed to observe the formation of different species during the pyrolysis and subsequent air-exposition (Figure 19). For Fe we could observe the formation of the metal structure and the subsequent reoxidation of the metal with the formation of magnetite. In contrast, in the NiPc, we could observe the formation of Ni, which seems to be more stable as its concentration does not change after the exposition to air, and no oxides were detected. All the results have finally been confirmed with the analysis and fitting of the EXAFS spectra.

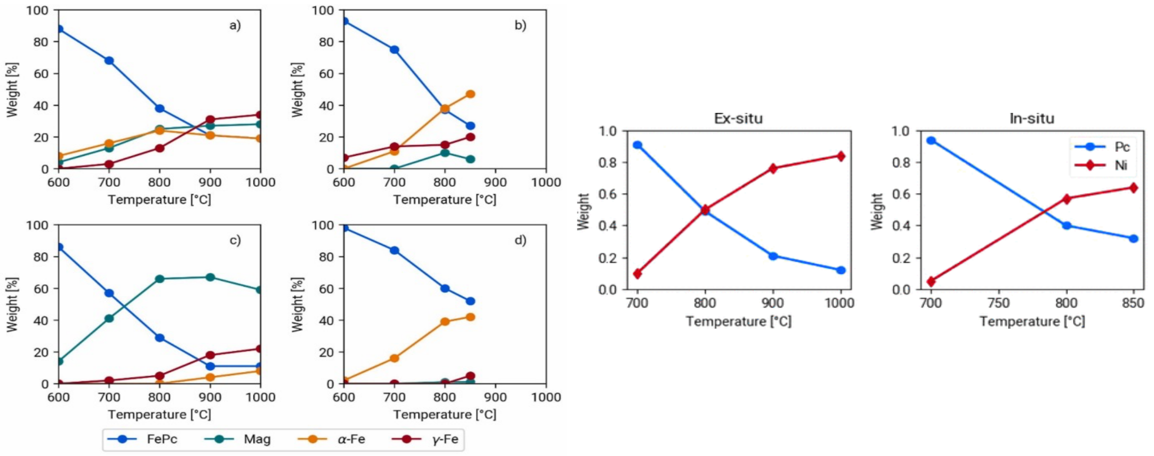

Figure 19: Results of the LCF. Left, FePc: a) data collected ex-situ in Ar/H_2 atmosphere, b) data collected in situ in Ar/H_2 atmosphere, c) data collected ex-situ in Ar atmosphere, d) data collected in situ in Ar atmosphere. Right, NiPc: In blue, the weight of the phthalocyanine component is shown, and in red, that of metallic nickel is shown.

Similarly, XAS was used to study different CuO-ZnO catalysts for CO_2Reduction Reaction [24-Peer]: after the analysis of fresh materials to assess the influence of the Cu/Zn ratio on the structure, operando measurements were carried out to observe structural changes occurring when different potentials are applied, using a custom-built cell provided by the users. Cu has shown reduction with the decrease of the applied voltage, and the various phases formed have been studied through LCF. Demonstrating the effectiveness of these materials opens the way to a reduced dependency on PGMs and the availability of environment-friendly materials for catalysis.

PGMs Electrocatalysis

Collaboration between user and staff

Platinum and Palladium have been deeply studied at the beamline, due to their importance in HER and ORR [21-Fracc, 24-He] processes. In particular, we would like to highlight the importance of the application of Fixed Energy X-ray Absorption Voltammetry (FEXRAV) measurements [22-Berr] as a method to realize operando experiments in the electrochemistry field. This technique is a mixed operando X-ray Absorption Spectroscopy/Electrochemical analysis that involves acquiring the X-ray absorption coefficient of an electrode subjected to electrochemical stimuli. The X-ray beam energy is held constant; the choice of energies was made considering the maximum variation of the absorption coefficients of the species expected to be formed at the target during electrochemical cycling (Figure 20).

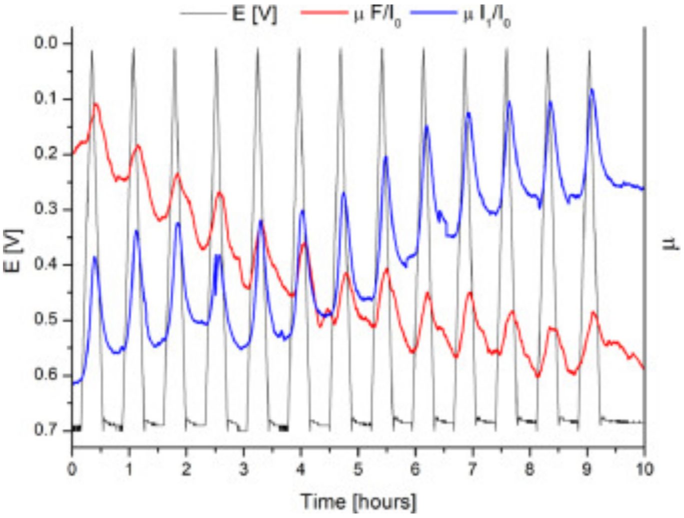

Figure 20: FEXRAV cycles. The variation of the Working Electrode potential (black) is coupled in time with the variation of the X-ray Absorption fluorescent signal (red) and the variation of the X-ray Absorption transmitted signal (blue).

By setting the right X-ray beam energy, it is then possible to determine the speciation of an element of choice, permitting the study of the transition between the metallic and ionic forms of a catalyst. In this experiment, FEXRAV was employed to evaluate the variations between Pd^0 and Pd^{2+} at the electrode (by sampling the fluorescence X-ray signal), and of the Pd^{2+} present into solution (by the acquisition of the transmitted absorption X-ray coefficient). The study of the working electrode in three different solutions allowed to observe that a) palladium subjected to anodic stimulus in KOH 2 M solution dissolves with the same rate when subjected to subsequent voltametric cycles, b) palladium subjected to anodic stimulus in KOH 2 M + EtOH 2 M undergoes an initial dissolution process once a certain particle size is reached. Having reached a certain particle dimension, the process slows down, eventually reaching a steady state (no dissolution, same trend is visible in both the half-cell experiments and the FC experiments), and c) no Pd mass loss was observed during anodic stressing in KOH 2 M + KCOOH 2 M.

However, sometimes, the volumes of interaction which are of interest in studying the electrochemical behaviour, and the subsequent changes occurring in the electrodes, are extremely shallow. For this reason, it may be necessary to perform analyses in Grazing Incident conditions [24-Berr]. In this experiment a GI-FEXRAV cell has been developed in collaboration with the beamline staff (Figure 21).

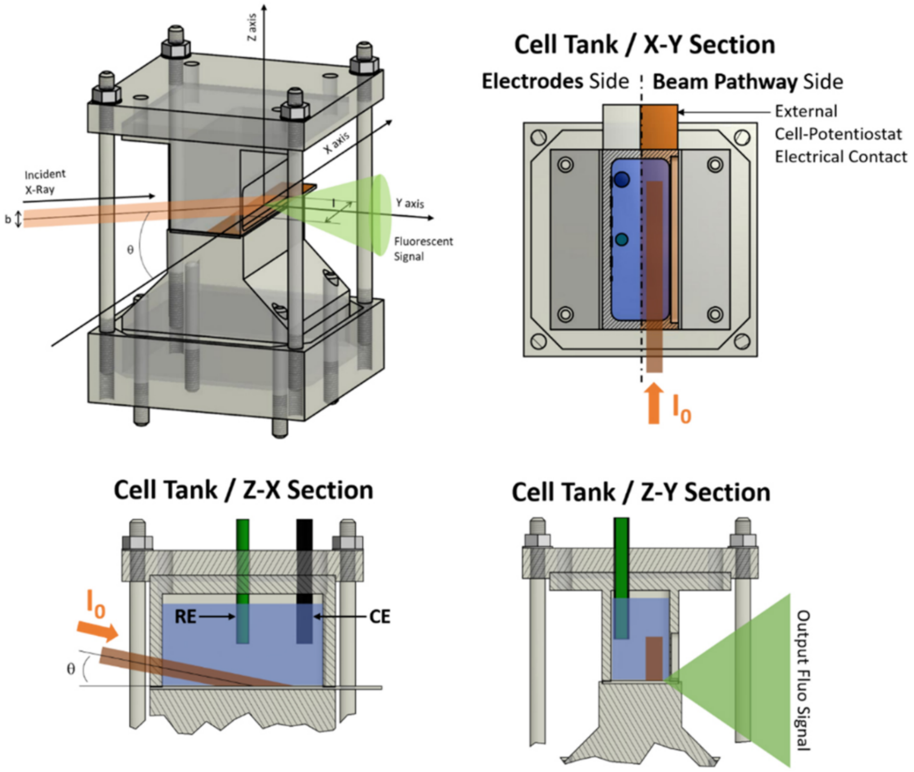

Figure 21: The rendering of the assembled cell from different sides and its working principles.

The GI-FEXRAV technique was tested on the three different Palladium-loaded Au electrodes. The use of different loadings of Pd on the Au base electrodes allowed to better describe the method and its present-stage limitations. A sample prepared with ultra-low Pd loading was useful to test the lower detection capability of the technique. The samples were not tested sequentially using GI-FEXRAV. The Intermediate Pd loading sample was examined on the BM08 beamline prior to ESRF-EBS upgrade, while the Low and High loading samples were examined on the same line after the accelerator refurbishment. At the present stage, it is possible to study Pd to PdO transition using effectively the GI-FEXRAV technique on the intermediate loading sample only, by monitoring its reversible oxidation. The Pd in the ultra-low loading sample was probed using Grazing Incidence XAS, *ex-situ*, *in-situ* and *operando*. The *ex-situ* acquisition was first performed to capture the initial situation of the ultra-thin Pd film. The same electrode was tested during an *operando* XAS, by assembling the EC cell in NaOH 2M and acquiring XANES spectra after static potential tests (30 min hold) at increasing potentials (0.05, 0.50 and 1.00 V vs. RHE). It was possible to acquire the edge jump of the Pd and, despite the noisy nature of these spectra, to notice the increase in intensity of the PdO peak (at about 24 370 eV) from the 0.05 V vs. RHE potential step to the 0.50 V vs. RHE. Finally, the operando test using the GI-FEXRAV was conducted by fixing the beam energy at 24 370 eV and by performing voltammetries with a scan speed of 1 mV/s; by analysing the trend of the absorption signal with the voltametric scan progression it was possible to observe the same decrease in the overall signal which (Figure 22) was visible for the Pd/C system [22-Berr] in the bare alkaline electrolyte.

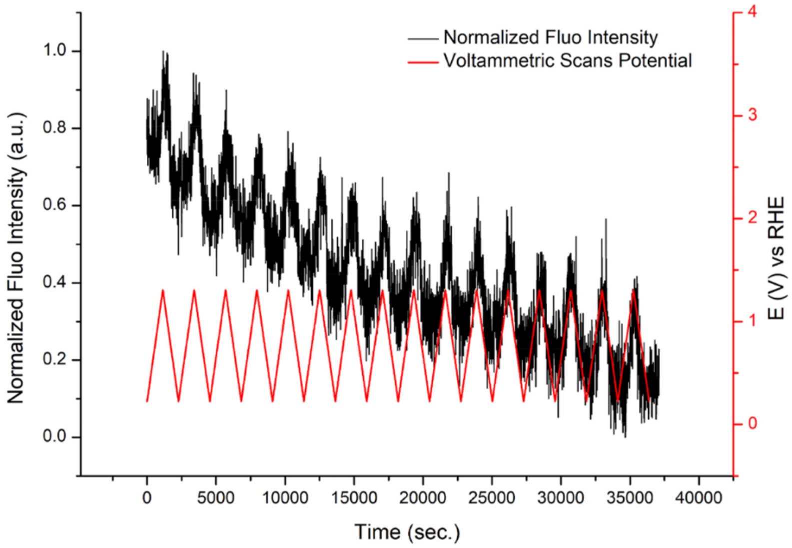

Figure 22: An image reporting all the GI-FEXRAV cycles, showing the overall decrease in the fluorescence absorption signal due to Pd dissolution at the electrode.

Energy Storage

User driven projects

Developing efficient materials for battery electrodes is of great importance today. At this purpose, operando XAS was employed to study new materials for energy storage. The study of de-/lithiation mechanisms in alternative lithium-ion battery electrode materials [20-Trap], i.e., carbon-coated) Fe- and Co-doped zinc oxide anodes, using pouch cells is an example. The operando measurements at the Co K-edge for $Zn_{0.9}Co_{0.1}O$ (Figure 23) show that cobalt is gradually reduced during the initial lithiation and essentially metallic at around 50% of the total discharge capacity. The reduction of zinc to the metallic state is completed slightly later, indicating that the reduction of cobalt during the conversion reaction is slightly preferred over the reduction of zinc. In the case of $Zn_{0.9}Fe_{0.1}O$–C, this effect is even more pronounced, and iron is completely reduced to the metallic state already at a rather early stage of the lithiation reaction, while zinc becomes metallic only at a much later stage.

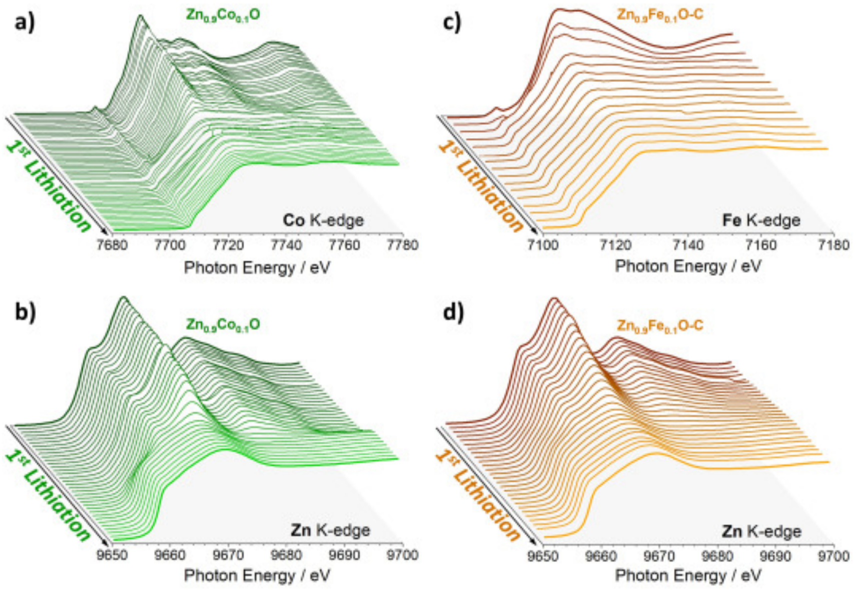

Figure 23: Operando XANES measurements for the first lithiation of electrodes based on (a,b) Zn0.9Co0.1O (in green) and (c,d) Zn0.9Fe0.1O–C (in orange): (a) Co K-edge, (b) Zn K-edge of Zn0.9Co0.1O, (c) Fe K-edge, and (d) Zn K-edge of Zn0.9Fe0.1O–C.

A similar approach [24-Xue], also using pouch cells was used to study the Nb oxidation state and local structural environment during the de/lithiation process. The operando XAS data for the Nb K-edge reveal a continuous shift of the pre-edge and edge position toward lower energies upon lithiation, and eventually disappearance of the pre-edge feature. This shift is well in line with the reduction of the niobium oxidation state because of the Li^+ insertion. Upon delithiation, this shift proved fully reversible.

Cultural Heritage

In the field of cultural heritage (CH), the beamline and the beamline staff are primarily working on the TEY application for sample characterization and degradation studies. Artifact degradation is a particularly sensitive topic, as understanding the underlying processes could not only help prevent it in museums but also pave the way for potential restoration efforts. The beamline staff has recently worked on the development of different anodes to analyse CH samples of various shapes and sizes and is defining a protocol to conduct not only spot analysis but also mapping. Indeed, mapping FY-TEY will allow one to spatially visualize the presence of different surface/bulk phases of degraded samples. As CH samples present a great inhomogeneity (lateral and in-depth) collecting 2-dimensional data of the surface and the bulk will give a great boost to the study of photochemical processes, as it will allow users to investigate not only the fully degraded region but also the lateral interfaces, with the possible presence of secondary or intermediate products. At present, the staff is working to implement this application in the study of lustre ceramic samples. These artifacts indeed present a superficial nanolayer of metallic nanoparticles (Cu and Ag), which covers a glaze containing oxides, and are being used as a benchmark to evaluate the limits and build a solid protocol of analysis.

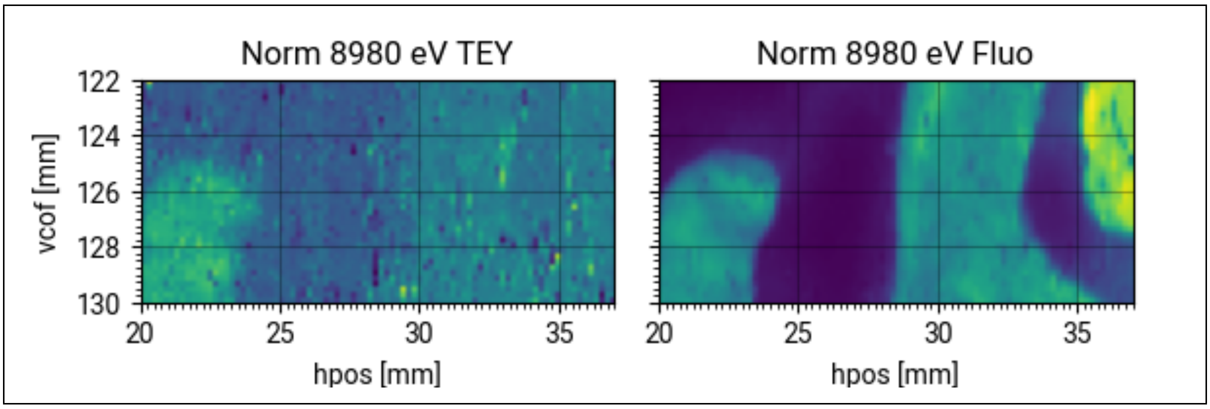

Figure 24: TEY and FY images of the copper edge of a region of a luster ceramic sample. The yellow regions represent the area with a high Cu signal. Is evident the difference between the TEY and Fluorescence maps as different region is highlighted.

Pigments degradation

Users and staff's projects

The coupling of FY and TEY measurements has been shown to be essential when studying the degradation processes of pigments. Indeed, these processes occur due to photochemical processes, affecting primarily the sample surface. For this reason, applying only fluorescence (or even worse, transmission) measurements may hinder the presence of the surface photodegradation products [23-Moni, 22-Moni]. This approach has been successfully applied to study the degradation processes of Cr pigments. The study was conducted on artificially aged mock-up pigments, the comparison of un-aged/aged and FY/TEY measurements has made it possible to observe the formation of Cr^{III} phases and calculate the phase concentrations. These results were also compared with data collected from lateral sections, showing a good agreement. The application of coupled FY/TEY is thus a great alternative, that, even though preventing a full in-depth profiling, allows for a fast and reliable approach in observing the degradation process, also as a screening protocol to easily select degraded samples for further studies.

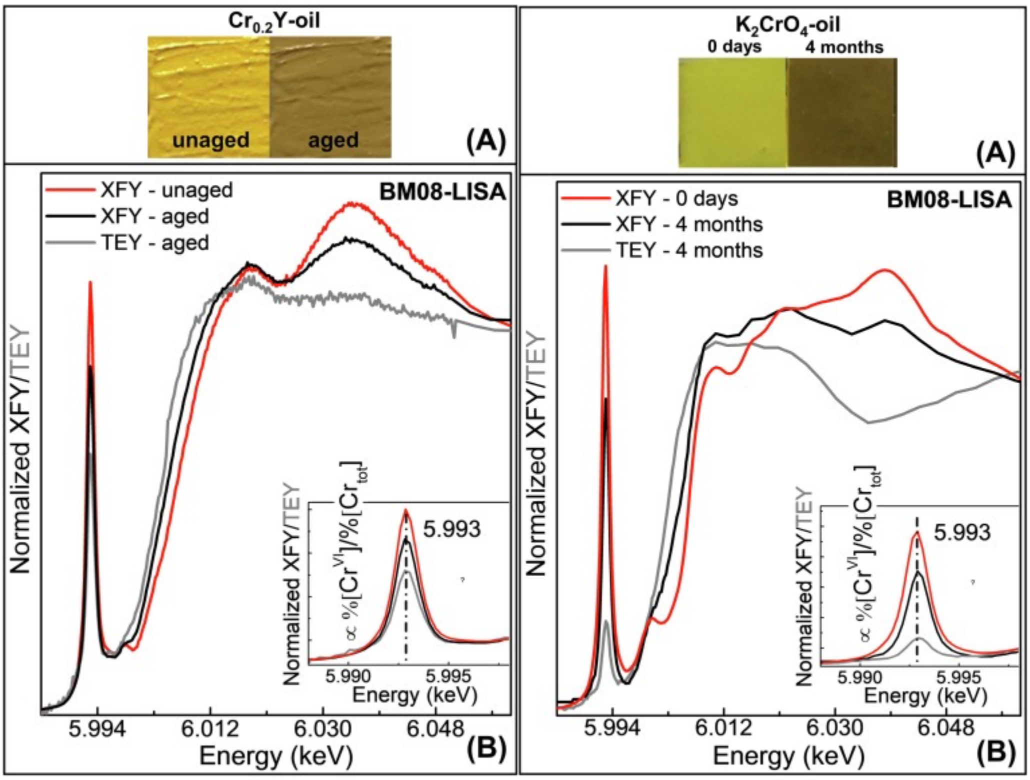

Figure 25: Left (A) Photographs of sulphate rich-chrome yellow type (PbCr0.2S0.8O4) paint mock-ups before (left) and after artificial aging with UVA-visible light (right). (B) Cr K-edge XANES spectra collected from the surface of unaged/aged Cr0.2Y paints

Environment

Several papers have been published in the field of environmental science. In most cases, the XAS analyses have been carried out on diluted samples benefiting from the focused beam, the high photon flux and the use of energy resolving detectors (HpGe, SDD) available at LISA.

Nanomaterials interaction with plants

User driven project

The impact on the environment of industrial process residues or fertilizers, and especially on crops, is highly relevant in the pursuit of more sustainable industrial practices. A relevant subject has been the study on nanomaterials performed by the group headed by M. Marmiroli (University of Parma) to shed light on the mechanism of uptake and metabolism in plants exposed to CdS quantum dots, used in LED screens and solar power cells [20-Marm] in view of possible decontamination strategies. Using EXAFS spectroscopy, the research revealed that CdS QDs are biotransformed in plants, highlighting a nanoscale-specific detoxification mechanism. A more recent work addressed the need to evaluate the biological impact of CuO nanoparticles as sustainable nanofertilizers in crops. [21-Marm]. In particular, CuO nanoparticles were shown to be non-toxic to plant reproduction and triggered distinct nanoscale-specific molecular responses.

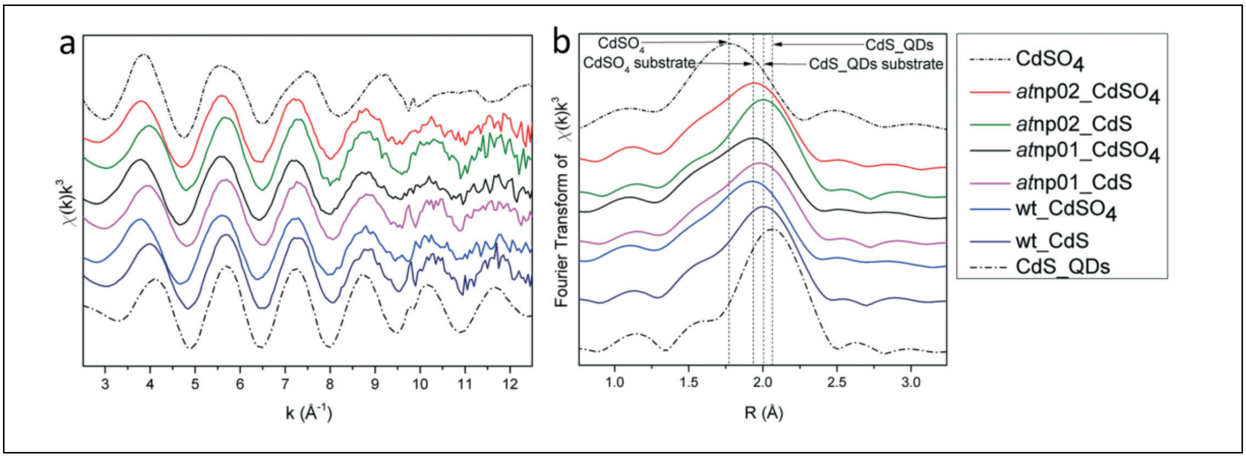

Figure 26: (a) EXAFS and (b) Fourier transform spectra of studied samples and reference compounds. For each reference the average is 2 scans, for the samples the average is 8 scans. Figure from [20-Marm]

In both studies the XAS analysis has permitted a characterization of the chemical state of the potentially polluting metal. Experiments have been performed in fluorescence mode with a focused beam due to the high dilution of these elements.

Metal speciation in the environment

User driven project

In the field of metal speciation in the environment, we report the study conducted by Petroselli et al. [20-Petr], who investigated the iron speciation in airborne particulate samples collected during different episodes of Saharan dust transport in comparison to mixed and non-Saharan (human origin) samples. The study was performed in fluorescence mode with a focused beam and the spectra have been acquired using a 12 element HP-Ge detector.

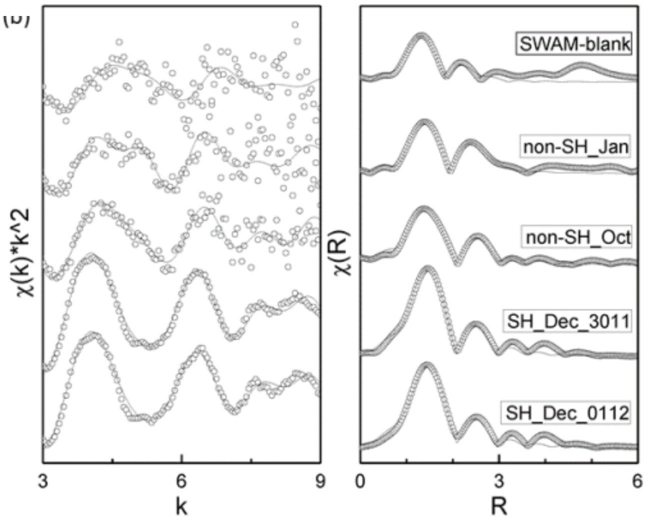

Figure 27: Left, EXAFS spectra of some Saharan samples, non-Saharan samples and blank filter. Right, Fourier transformed spectra

The XAS analysis revealed a predominance of Fe(III) in 6-fold coordination for Saharan dust while a shift towards Fe(II) and four-fold coordination occurred in mixed and non-Saharan samples. This work clarifies Fe speciation trends across dust types and offers a means to distinguish natural from anthropogenic fine particles.

Detection and removal of pesticides

User driven project

An innovative study has been performed by Kalinic et al. [22-kali]. The team investigated the formation mechanism of Co_3O_4 nanopetals on Si-based photoanodes through the thermal oxidation of a deposited metallic cobalt film. XAS measurements performed in fluorescence mode after thermal air-annealing for definite time intervals confirmed the formation and growth of the nanopetals. Indeed, as clearly shown in Figure 28, the XANES spectra of a 50 nm thick film change from metallic Co to Co_3O_4 with increasing annealing time. Furthermore, the study demonstrates their potential for photoelectrochemical sensing and degradation of fenitrothion (FNT), a commonly used organophosphate pesticide which represents a serious risk to public health.

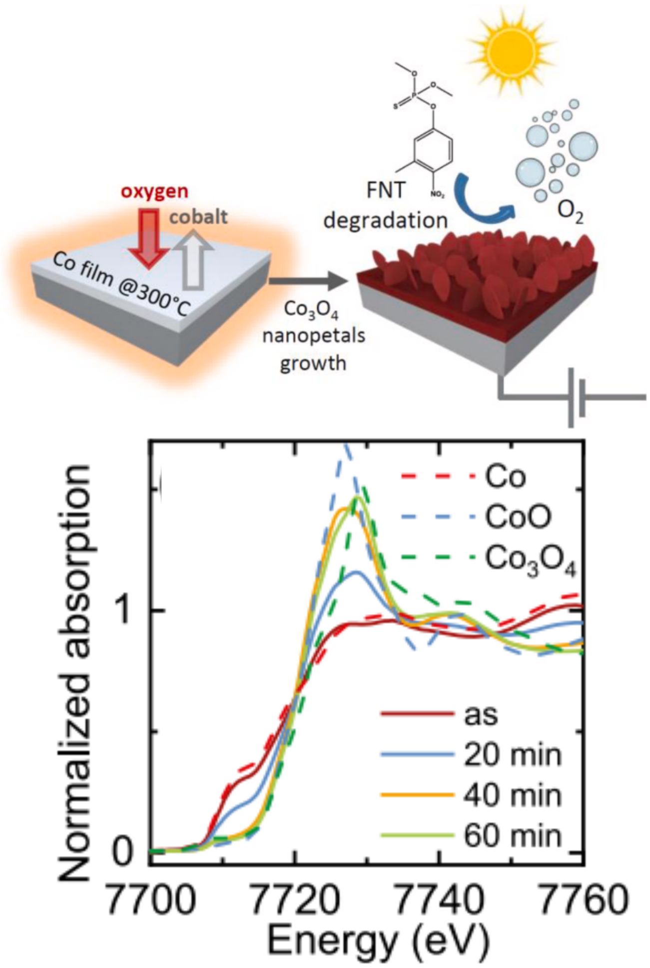

Figure 28: XANES spectra of a Co 50 nm-thick deposited film annealed in air at 300 ◦C for different time intervals. The sketch above is a graphical abstract of the paper. Taken from [22-kali]

Silver recovery from solar cells waste

User driven project

In the framework of a collaboration with an Italian company (Orim) and the group headed by G. Giuli (University of Camerino), a study was performed to develop an innovative process to recover silver from silicon solar cell waste. The study explores a novel approach using hydrometallurgical leaching and an electrochemical electrodeposition-redox replacement (EDRR) method to recover silver with high purity. XAS analysis played a crucial role in studying the oxidation state of copper, which plays a key role as sacrificial metal in the EDRR process. The XANES spectra of Cu-solar cell in blue (Figure 29) displays edge energy peak positions and relative peak intensities which are compatible with that of metallic copper, thus indicating that copper is mainly in the metallic state and not as an oxide.

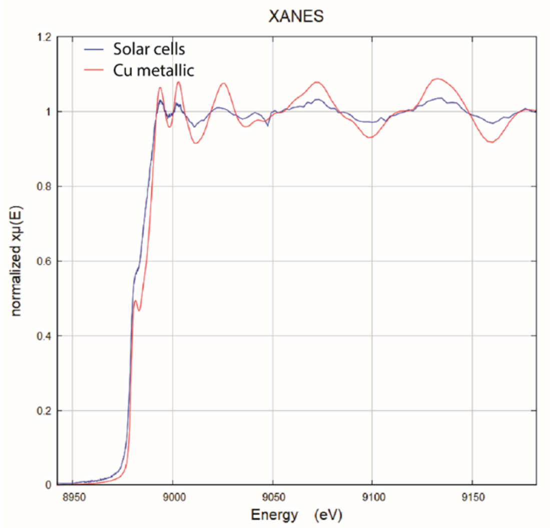

Figure 29: XANES Spectra of solar cell waste at Cu K-edge.

Geology

The geology research was mainly focused on the structural characterization of recently discovered minerals and natural glasses. XAS was employed as a complementary technique providing key information about the elemental chemistry and local structure. The studies profited from the high photon flux (see table 1) focused beam, and the use of energy resolved fluorescence detectors (SDD and HP-Ge).

Minerals and natural glasses geochemistry

User driven projects

Several studies explored the geochemistry of minerals and natural glasses. Lepore et al. [22-Lepo1] investigated lanthanum (La) ions hosted in montmorillonite to shed light on the structural location of the La ions, whether they are incorporated in the structure or adsorbed at the surface. With Rare Earth Elements (REE) recycling gaining importance, the mechanisms behind La uptake in clays—especially the role of surface vs. structural interactions—remained unclear. XAS measurements, performed in fluorescence mode with the 12-element HP-Ge detector, showed a similar La local environment in all the samples studied and a La – O coordination shell like that of hydrated La ions in aqueous solution. Overall, the XAS analysis evidenced a complex structural mechanism of La uptake providing important and accurate information for the improvement of the existing methods and for the exploration of new technologies for REEs recovery.

Biagioni et al. [20-Biag] investigated thallium (Tl)-bearing alum-(K) and voltaite from the Fornovolasco mining complex in the Apuan Alps (Tuscany, Italy). Thallium is a toxic metal pollutant commonly associated with K-bearing minerals due to its geochemical similarities with potassium (K) and rubidium (Rb). Tl had previously been detected in the public tap water of the area [C. Biagioni et al 2017, DOI: 10.1016/j.scitotenv.2017.02.177] , posing a significant risk to public health. The study explores the role of K-sulfates in temporarily sequestering Tl in acid mine drainage environments. XAS played a crucial role in characterizing the oxidation state, local coordination environment, and bonding behaviour of Tl. The XAS spectra at Tl L_3-edge (12658 eV) were collected in fluorescence mode by means of a 12-element solid state detector (HP-Ge).

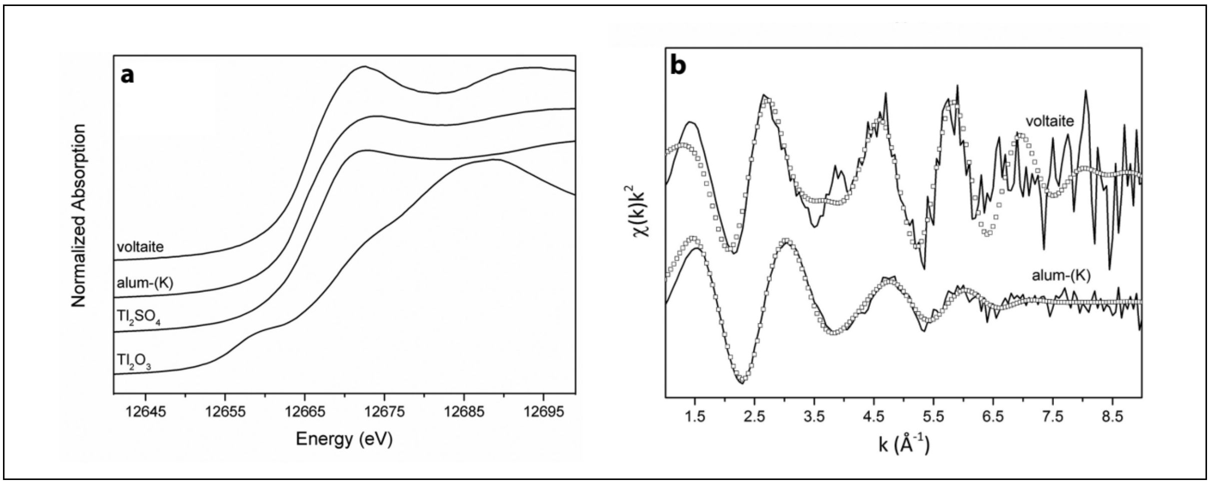

Figure 30: (a) Normalized Tl L3-edge XANES for alum-(K), voltaite, and model compounds. (b) Tl L3-edge EXAFS. Taken from [20-Biag].

XANES analysis confirmed that Tl occurs as Tl^+ in both Alum-(K) and Voltaite, with the XANES region fairly resembling that of Tl_2SO_4 reference (Figure 30 a). EXAFS analysis confirmed that Tl partially substitutes K, showing the presence of Tl^+ in 6-fold coordination with O for both minerals. This work reveals how alum-(K) and voltaite can transiently sequester Tl^+ through specific crystal-chemical mechanisms, opening the way to strategies to monitor and mitigate Tl pollution in mine drainage environments

Koeberl et al. [22-Koeb] performed a comprehensive study of 18 natural glass samples from Belize. For the XAS characterization, measurements have been taken at the Fe K-edge (7112 eV) in fluorescence mode at high resolution with the Si(311) crystal pair. The XANES analysis revealed a low oxidation state for iron, predominantly Fe^{2+}, consistent with formation under highly reducing conditions, which is a characteristic feature of known tektites. This supports an impact origin rather than a volcanic one, as volcanic glasses typically display higher oxidation states (more Fe^{3+}).

Characterization of recently discovered minerals

User driven projects

In a recent paper, Cámara et al. [23-Cama] performed a comprehensive characterization of Piccoliite, a newly discovered manganese arsenate mineral found in two locations in Piedmont, Italy: the Montaldo di Mondovì mine and the Valletta mine. XAS at Mn K-edge was employed to study the oxidation state and local atomic environment of manganese. The measurements were performed in fluorescence mode with the 4-channel SDD detector ARDESIA.

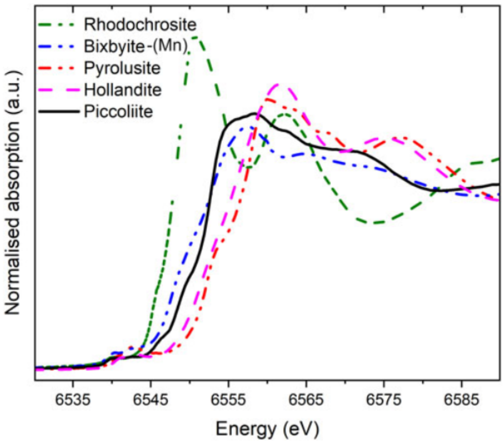

Figure 31: Mn K-edge XANES of piccoliite from Valletta mine, together with rhodochrosite, bixbyite-(Mn), pyrolusite and hollandite. Taken from [23-Cama].

The XANES analysis suggested the presence of both Mn^{3+} and Mn^{4+}, especially in the Valletta mine specimens, as shown in Figure 31. EXAFS analysis showed that Mn occupies a highly distorted octahedral site.

Photoelectrochemical water splitting

Collaboration between staff and users

Research on solar-driven water splitting is crucial for advancing clean hydrogen production, offering a sustainable alternative to fossil fuel-based methods. By harnessing sunlight to generate hydrogen, this technology holds the potential to significantly reduce carbon emissions and support the transition to a green energy economy. LISA has been particularly active in the field of photoelectrochemical water splitting (PEC-WS) thanks to its efficient instrumentation for diluted systems. Several papers have been published resulting from collaboration with Italian universities (University of Milano, University of Pavia, University of Bologna). The main objective is the search for suitable electrode materials for the development of PEC cells. Among the promising materials copper oxide [20-Visi] and ligand Cu complexes [24-Amth] have been investigated. Another promising material which has been extensively studied is $WO_3/BiVO_4$ heterostructure coated with cobalt iron oxide (CoFeOx) or cobalt-iron Prussian blue overlayers [24-Vecc]. In most of the cases XAS measurements were carried out on custom made PEC cells in operating conditions, specifically designed to allow for XAFS analysis. Moreover, the effect of sunlight-equivalent illumination and voltage bias has been investigated by either performing fixed potential spectroscopy, or fixed X-ray energy absorption voltammograms (FEXRAV). To this purpose, a tailored algorithm for point-by-point acquisition triggered light stimulus has been implemented at LISA to achieve time-gated acquisition.

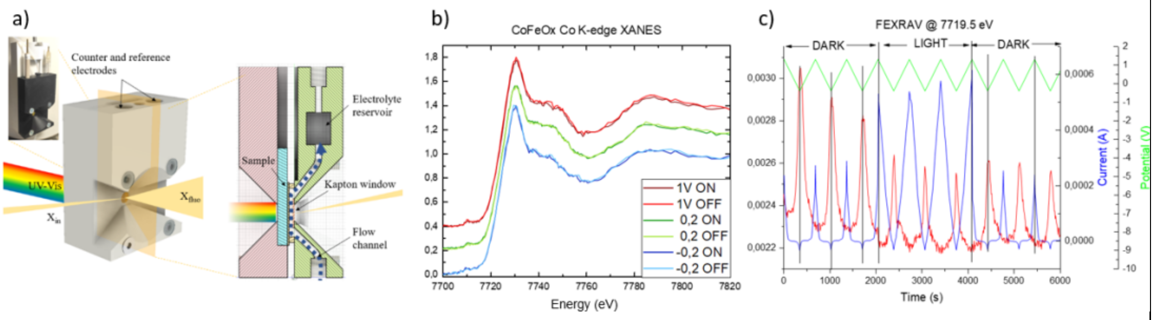

Figure 32: a) 3D-printed custom PEC cell scheme; b) fixed potential XAS spectra in dark/light conditions at CoK-edge; c) FEXRAV @7719.5eV in dark/light conditions.

Internal projects

LISA is involved in several projects that make it possible to develop its scientific programmes:

CECOMEC

The CECOMEC project (https://cecomec.wordpress.com) is funded by CERIC and it is focused on the study of new materials for Solid Oxide Fuel Cells and Electrochemical cells based on cerium oxide doped with additional lanthanides of transition metals. The activities are carried out in collaboration with two Polish institutions: the Gdansk Tech and the SOLARIS synchrotron. The project supports one postdoctoral position plus consumables for the activity and uses X-ray Absorption Spectroscopy to analyse the incorporation site of the dopants in the ceria host matrix.

NEST

The NEST project (https://fondazionenest.it) is one of the projects funded by the Italian “Piano Nazionale di Ripresa e Resilienza” (PNRR) and involves a major consortium of Italian universities, and research institutes. It is focused on the sustainable energy transition and in its framework, LISA is active in the so-called “Spoke 4 “(Clean Hydrogen and Final Uses). LISA carries out the structural characterization of electrodes for Solid Oxide Fuel Cells based on perovskite-type materials.

PON - Doctorate with Industry

LISA collaborates with the Pavia University and the “Industrie De Nora SpA” company for conducting XAS measurements for a doctoral thesis. In particular, the studies are focused on Ni and Ni-based electrodes for hydrogen production by water electrolysis. The project is financed by the Italian PON (Piano Operativo Nazionale – Ricerca e Innovazione 2014-2020) via an action focused on doctorates on “green topics”.

Agreement with Uni-Bo

An agreement with the Bologna Alma Mater University has been signed for strengthening the collaboration in the field of photo-catalysis with the XAS technique. The agreement funds a position of researcher (RTD-A) at the university that spends several months at the beamline, supporting the staff and carrying out IHR programs.

Agreement with Uni-MiB

An agreement with the Milano-Bicocca University has been signed for fostering the research in the fields of fuel cells (studies on pyrolyzed phthalocyanines of different transition metals) and cultural heritage such as surface elemental mapping and degradation of pigments, through the XAS technique.

5. Future perspectives and plans for further development of the beamline for an optimal exploitation of the ESRF EBS

For the forthcoming years, the activity at LISA will be focused on research lines of great interest and for which the source and the beamline possess the highest potential. The new EBS ring brings a series of aspects that open the way to new experimental opportunities. Mainly, these include:

- High brilliance
- High (spatial, temporal) stability
- Time modes

It must be considered that with the recent upgrade of the X-ray optics LISA provides now a very stable, intense and small beam making it ideal for

- Pump and probe studies
- Operando studies
- Surface studies
- Mapping

The first category is a highly relevant subject as here we find the broad research linked to photo-electro-chemistry. The research on materials for solar light harvesting is a particularly strategic topic now, and LISA possesses some strong points for carrying out research in this topic:

i) the EBS source provides time modes ideal for experiments in the range of 1-100 ns. This range is interesting as the light sensitizers should possess long-lived (ns range) excited states to be effective for photocatalysis.

ii) LISA is a bending magnet beamline so the beam is sufficiently intense to allow the collection of data of good quality while also limiting the radiation damage on the sample.

iii) The small and stable beam of LISA on the sample has a size well adapted for acting as a source in an emission spectrometer.

iv) At present, lasers with a high repetition rate are available to exploit every flash from the machine (namely in 16b mode) for data collection.

Thus, appropriate funding will be sought in the near future to establish a laser station coupled with a HERFD spectrometer allowing pump and probe experiments in both conventional fluorescence XAS and High-Resolution Fluorescence, particularly critical in the analysis of compounds based on 4d or 5d metals.

Concerning experiments in operando mode, the development of XAS data collection in continuous mode will constitute a major advance. This has already been pioneered with the present instrumentation and will be realized in a more effective way as soon as the BLISS environment will be available and new electrometers for reading the ion chambers/photodiodes. This will improve the research on catalysis, batteries, phase change and can be realized with moderate financial support. Considering the present monochromator the time range that could be addressed is in the order of tens of seconds – minutes.

Regarding surface studies, particularly effective in the investigations on materials for microelectronics or model catalysts, the exceptional characteristics of the beam (small size and stability in energy) make LISA an ideal beamline for the investigations on thin films in Grazing Incidence Geometry. The collection of data with the polarization vector parallel and perpendicular to the surface is possible and can provide a detailed description of the material under analysis. The present sample manipulator does not allow in a simple way this kind of measurements and a new manipulator with

i) the possibility of appropriately orient the sample with respect to the polarization vector.
ii) An anode for the collection of TEY data.

will be necessary.

For what concerns mapping a considerable advance would be the adoption of a microfocusing system, with polycapillary optics. This solution would be of simple implementation and would have a moderate impact on the experimental station in EH2, whereas providing a focal spot of a few μm. For this experimental technique, the adoption of fast (continuous) scanning offered by BLISS will be beneficial to reduce the collection time.

For all these activities a significant improvement would be the purchase of a new fluorescence detector which will need a dedicated funding.

As a final point, internal funding will be searched for the renewal of some critical components (main slits, attenuators, beam shutters, lamellar bellows) whose failure would severely impact the beamline operation.

A list of the major proposed evolutions of the beamline is given below:

XAS – photophysics	If funding is available, installation of a high repetition rate (MHz) power laser (class 3B or 4) in the visible range for time resolved (ns) studies for solar-based electrochemistry.
HERFD	If funding is available, an emission spectrometer for HERFD will be installed for improving the data collection on • highly diluted systems • systems involving 4d, 5d elements with highly broadened absorption edges systems with superimposing emission lines.
XAS – operando experiments	Development of continuous scan for fast (tens of seconds, minutes) data acquisition. This will be possible with the adoption of the BLISS environment for the beamline management, foreseen in the late 2025-early 2026 period. The adoption of the new electrometers under development at ESRF and optimized for transient measurements will be necessary for this purpose. This will foster the research on materials in operando conditions like fuel cells and batteries and could be an interesting opportunity for industrial research.
Surface studies	New manipulator for Fluorescence / TEY data collection with possibility of orienting

	the sample surface with respect to the X-ray polarization vector
Microfocusing	Polycapillaries for generating a micron-sized beam for mapping or micro-XAS.

6. Conclusion

The period 2020-2024 has been critical for the activity of LISA. On one hand we have benefited from both the new storage ring and the new X-ray optics with a considerable improvement of the experimental perspectives of the instrument. On the other hand, the pandemic period has severely impacted the activity of the users as well as some major failures of the instrumentation. Nonetheless, the beamline has remained highly active and has fulfilled its commitments to beam delivering with a considerable production of science and publications.

The collaboration with CERIC-ERIC has brought new communities, scientific topics and staff and a full team of scientists has enabled the boost the In-House Research program.

For future projects, it will be necessary to secure external funding, which the scientific staff will actively pursue.

7. Publications

As stated in the previous sections, LISA has been undergoing a difficult period in 2020 because of the joint effect of the beamline refurbishment (2017-2018), the ESRF shutdown (2019) and the pandemic (2020-2021). The users' activity and productivity were affected as a consequence. Figure 33 shows the publications produced by LISA in the period 2020-2024. A drop is evident in 2021 generated by the joint effect of the events just mentioned but since 2022 the publications have been progressively increasing denoting recovery of activity. Note also the equilibrium between publications to which the staff contributed and those authored independently by the users.

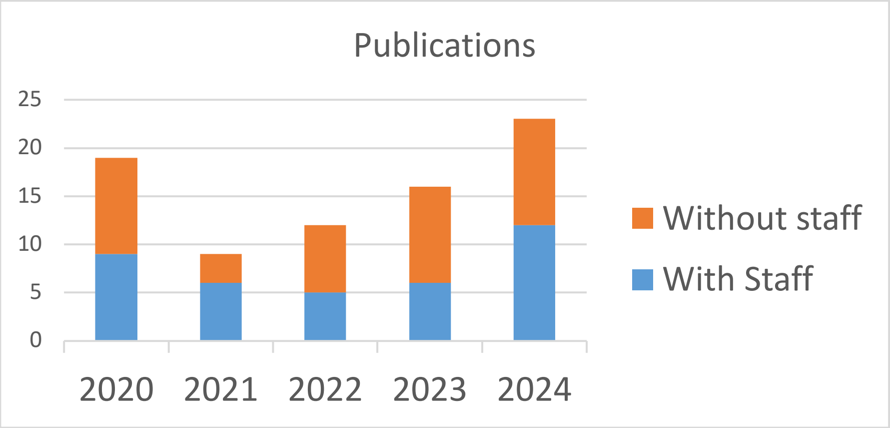

Figure 33: Publications per year dividing those with and without staff members among the authors.

Figure 34 shows the Impact Factor of Journals where the LISA works are published. There is a peak around 4-6 showing the good quality of the publications.

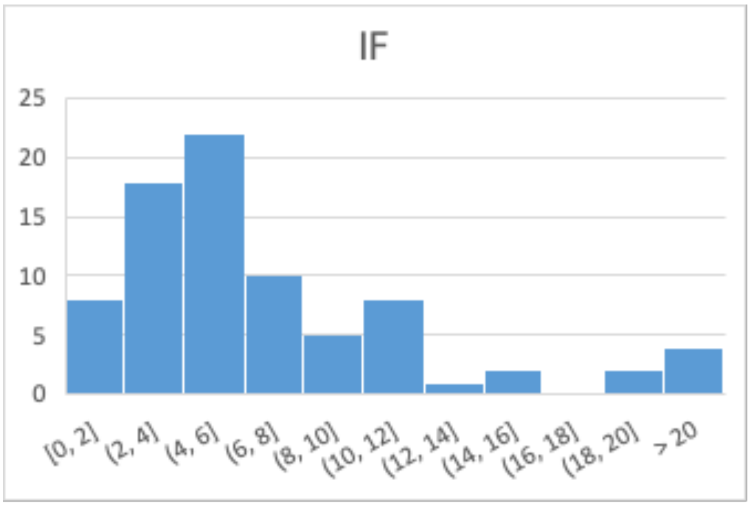

Figure 34: Distribution of the Impact factor values of the journals where the LISA publications of 2020-2024 have appeared.

It is worth recalling that LISA publishes yearly an annual report under the title "Activity report of the Italian CRG beamline at the European synchrotron radiation facility (ESRF)" with ISSN 2553-9248 whose issues can be found either on the CNR-IOM site (https://www.iom.cnr.it/p/gilda-reports) or on the Zenodo repository. The latest issues can be found at the following links:

- Annual report 2024
- Annual report 2023
- Annual report 2022
- Annual report 2021
- Annual report 2020

The reports detail the latest technical updates of the beamline, as well as the most relevant results by the users or the students who have spent time at LISA.

The complete list of publications for the period 2020-2024 is presented here. First are the 10 most cited followed by the remaining ones. A detailed analysis reveals an H-index of about 12 for these publications at the present date.

10 most cited publications

1. [20-Noe] Noé P., Verdy A., d'Acapito F., Dory J.B., Bernard M., Navarro G., Jager J.B., Gaudin J., Raty J.Y. - Toward ultimate nonvolatile resistive memories: The mechanism behind ovonic threshold switching revealed Science Advances 6, eaay2830-1-eaay2830-11(2020) 89 citations https://doi.org/10.1126/sciadv.aay2830
2. [20-Fant] Fantin A., Lepore G.O., Manzoni A.M., Kasatikov S., Scherb T., Huthwelker T., d'Acapito F., Schumacher G. - Short-range chemical order and local lattice distortion in a compositionally complex alloy Acta Materialia 193, 329-337(2020) 62 citations https://doi.org/10.1016/j.actamat.2020.04.034
3. [20-Dora] D'Orazio M., Campanella B., Bramanti E., Ghezzi L., Onor M., Vianello G., Vittori-Antisari L., Petrini R. - Thallium pollution in water, soils and plants from a past-mining site of Tuscany: Sources, transfer processes and toxicity Journal of Geochemical Exploration 209, 106434-1-106434-14(2020) 54 Citations https://doi.org/10.1016/j.gexplo.2019.106434
4. [20-Ma] Ma Y., Ma Yu., Giuli G., Euchner H., Gross A., Lepore G.O., d'Acapito F., Geiger D., Biskupek J., Kaiser U., Schütz H.M., Carlsson A., Diemant T., Behm R.J., Kuenzel M., Passerini S., Bresser D. - Introducing highly redox-active atomic centers into insertion-type electrodes for lithium-ion batteries Advanced Energy Materials 10, 2000783-1-2000783-13(2020) 37 citations https://doi.org/10.1002/aenm.202000783
5. [20-Tada] Tadayon M., Younes-Metzler O., Shelef Y., Zaslansky P., Rechels A., Berner A., Zolotoyabko E., Barth F.G., Fratzl P., Bar-On B., Politi Y. - Adaptations for wear resistance and damage resilience: Micromechanics of spider cuticular "tools" Advanced Functional Materials 30, 2000400-1-2000400-13(2020) 37 citations https://doi.org/10.1002/adfm.202000400
6. [20-Marm] Marmiroli M., Lepore G.O., Pagano L., d'Acapito F., Gianoncelli A., Villani M., Lazzarini L., White J.C., Marmiroli N. - The fate of CdS quantum dots in plants as revealed by extended X-ray absorption fine structure (EXAFS) analysis Environmental Science: Nano 7, 1150-1162(2020) 23 Citations https://doi.org/10.1039/C9EN01433K
7. [21-Marm] Marmiroli M., Pagano L., Rossi R., De la Torre-Roche R., Lepore G.O., Ruotolo R., Gariani G., Bonanni V., Pollastri S., Puri A., Gianoncelli A., Aquilanti G., d'Acapito F., White J.C., Marmiroli N. - Copper oxide nanomaterial fate in plant tissue: Nanoscale impacts on reproductive tissues Environmental Science and Technology 55, 10769-10783(2021) 20 citations https://doi.org/10.1021/acs.est.1c01123
8. [24-Muhy] Muhyuddin M., Berretti E., Mirshokraee S.A., Orsilli J., Lorenzi R., Capozzoli L., d'Acapito F., Murphy E., Guo S., Atanassov P., Lavacchi A., Santoro C. - Formation of the active site structures during pyrolysis transformation of Fe-phthalocyanine into Fe-Nx-C electrocatalysts for the oxygen reduction reaction

Applied Catalysis B: Environmental 343, 123515-123515-17(2024) 16 Citations https://doi.org/10.1016/j.apcatb.2023.123515

9. [20-Mala] Malara F., Fracchia M., Kmentová H., Psaro R., Vertova A., Oliveira de Souza D., Aquilanti G., Olivi L., Ghigna P., Minguzzi A., Naldoni A. - Direct observation of photoinduced higher oxidation states at a semiconductor/electrocatalyst junction ACS Catalysis 10, 10476-10487(2020) 14 citations https://doi.org/10.1021/acscatal.0c02789
10. [20-Rezv] Rezvani S.J., Mijiti Y., Gunnella R., Nobili F., Trapananti A., Minicucci M., Ciambezi M., Bresser D., Nannarone S., Passerini S., Di Cicco A. - Structure rearrangements induced by lithium insertion in metal alloying oxide mixed spinel structure studied by X-ray absorption near-edge spectroscopy Journal of Physics and Chemistry of Solids 136, 109172-1-109172-8(2020) 14 citations https://doi.org/10.1016/j.jpcs.2019.109172

---

11. [20-Daca] d'Acapito F., Kowalczyk P., Raty J.Y., Sabbione C., Hippert F., Noé P. - Local structure of $[(GeTe)_2/(Sb_2Te_3)_m]_n$ super-lattices by X-ray absorption spectroscopy Journal of Physics D 53, 404002-1-404002-8(2020) 12 citations
12. [21-Trap] Trapananti A., Eisenmann T., Giuli G., Mueller F., Moretti A., Passerini S., Bresser D. - Isovalent vs. aliovalent transition metal doping of zinc oxide lithium-ion battery anodes — in-depth investigation by ex situ and operando X-ray absorption spectroscopy Materials Today Chemistry 20, 100478-1-100478-10(2021) 12 citations

Other publications

13. [24-Amth] Amthor S., Ranu K., Bellido C.G., Salomón F.F., Piccioni A., Mazzaro R., Boscherini F., Pasquini L., Gil-Sepulcre M., Llobet A. - Robust molecular anodes for electrocatalytic water oxidation based on electropolymerized molecular Cu complexes Advanced Materials 36, 2308392-1-2308392-7(2024)
14. [24-Berr] Berretti E., Giaccherini A., Dell'Aquila V., Di Benedetto F., Montegrossi G., Lepore G.O., Innocenti M., d'Acapito F., Vizza F., Lavacchi A. - In-situ and operando Grazing Incidence XAS: a novel set-up and its application to model Pd electrodes for alcohols oxidation Pure and Applied Chemistry 96, 493-509(2024)
15. [24-Capo] Capobianchi A., Imperatori P., Cannas C., Rusta N., Locardi F., Slimani S., Ferretti M., Peddis D., d'Acapito F., Tauanov Z., Laureti S., Varvaro G. - Extending the Pre-ordered Precursor Reduction strategy to L10 ternary alloys: The case of MnFePt Journal of Alloys and Compounds 1008, 176650-1-176650-9(2024)
16. [24-Daca] d'Acapito F., Rehman M.A. - Effectiveness of ab initio molecular dynamics in simulating EXAFS spectra from layered systems Journal of Synchrotron Radiation 31, 1078-1083(2024) 1 citation
17. [24-Deam] De Amicis G., Testolin A., Cazzaniga C., d'Acapito F., Minguzzi A., Ghigna P., Vertova A. - In-situ surface activation of polycrystalline LaNiO3 electrocatalyst for the oxygen evolution reaction International Journal of Hydrogen Energy 87, 890-901(2024)
18. [24-Duck] Ducka A., Blaszczak P., Zajac M., Mizera A., d'Acapito F., Bochentyn B. - Limited dissolution of transition metals in the nanocrystalline cerium (IV) oxide Ceramics International 50, 50921-50933(2024)
19. [24-Fant] Fantin A., Lepore G.O., Widom M., Kasatikov S., Manzoni A.M. - How atomic bonding plays the hardness behavior in the Al–Co–Cr–Cu–Fe–Ni high entropy family Small Science 4, 2300225-1-2300225-12(2024) 1 citation
20. [24-Fant1] Fantin A., Manzoni A.M., Springer H., Kamachali R.D., Maass R. - Local lattice distortions and chemical short-range order in MoNbTaW Materials Research Letters 12, 346-354(2024) 2 citations

21. [24-Guer] Guerrini M., Magnaghi L.R., Fracchia M., Riccardi M.P., Pigoni G., Debbi G., Patrini M., Biesuz R., Tarantino S.C., Tamburini U.A., Ghigna P. - Minimizing the cobalt content in black ceramic pigments by Design of Experiments Ceramics International 50, 51181-51191(2024)
22. [24-Xe] He X., Fracchia M., Coduri M., Scavini M., Ghigna P., Marelli M., Della Pergola R., Vertova A., Minguzzi A. - Structure and activity of carbonyl cluster-derived PtFe nanoparticles as electrocatalysts for the oxygen reduction reaction in alkaline media ACS Applied Energy Materials 7, 1561-1572(2024)
23. [24-Masp] Maspero A., Bardelli F., Konidaris K.F., Uboldi M., Lucarelli C., Schiaroli N., Vitillo J.G. - Unraveling transfer hydrogenation mechanisms by ammonia borane to alkenes over self-healing copper nanoparticles: The complementary role of N-H bond, surface, and solvent ACS Catalysis 14, 9594-9606(2024)
24. [24-Mirs] Mirshokraee S.A., Muhyuddin M., Pianta N., Berretti E., Capozzoli L., Orsilli J., d'Acapito F., Viscardi R., Cosenza A., Atanassov P., Santoro C., Lavacchi A. - Ni-phthalocyanine derived electrocatalysts for oxygen reduction reaction and hydrogen evolution reaction: Active sites formation and electrocatalytic activity ACS Catalysis 14, 14524-14538(2024)
25. [24-More] Morelli M.B., Caviglia M., Santini C., Del Gobbo J., Zeppa L., Del Bello F., Giorgioni G., Piergentili A., Quaglia W., Battocchio C., Bertelà F., Amatori S., Meneghini C., Iucci G., Venditti I., Dolmella A., Di Palma M., Pellei M. - Copper-based complexes with adamantane ring-conjugated bis(3,5-dimethyl-pyrazol-1-yl)acetate ligand as promising agents for the treatment of glioblastoma Journal of Medicinal Chemistry 67, 9662-9685(2024)
26. [24-Ostro] Ostroman I., Vallana N., Marchionna S., Gentile A., Ferrara C., Pellini I.C., Fracchia M., Pianta N., Ruffo R. - Oxidized Ti3Al(1-x)SnxC2 MAX phases as negative electrode materials for sodium ion batteries Journal of Power Sources 624, 235543-1-235543-12(2024)
27. [24-Peer] Peerlings M.L.J., Han K., Longo A., Helfferich K.H., Ghiasi M., de Jongh P.E., Ngene P. - Synthesis and catalytic performance of bimetallic oxide-derived CuO–ZnO electrocatalysts for CO2 reduction ACS Catalysis 14, 10701-10711(2024) 4 Citations
28. [24-Real] Reale P., Pinto V., Cayado P., Celentano G., Armenio A.A., Rufoloni A., Santoni A., d'Acapito F. - Evidence of Gd substitution for Y in YBCO films with Gd excess Journal of Alloys and Compounds 983, 173921-1-173921-7(2024)
29. [24-Riva] Riva L., Dotti A., Iucci G., Venditti I., Meneghini C., Corsi I., Khalakhan I., Nicastro G., Punta C., Battocchio C. - Silver nanoparticles supported onto TEMPO-oxidized cellulose nanofibers for promoting Cd2+ cation adsorption ACS Applied Nano Materials 7, 2401-2413(2024) 1 citation
30. [24-Romo] Romolini G., Sun L., Fron E., Acapito F., Grandjean D., Roeffaers M.B.J., Martin C., Hofkens J. - Single atom silver-phosphors in titanosilicate matrix for enhanced LED applications Advanced Optical Materials 12, 2301894-1-2301894-10(2024) 1 citation
31. [24-Russ] Russo R.E., Awais M., Fattobene M., Santoni E., Cavallera R., Zamponi S., Conti P., Berrettoni M., Giuli G. - Silver recovery from silicon solar cells waste by hydrometallurgical and electrochemical technique Environmental Technology & Innovation 36, 103803-1-103803-12(2024)
32. [24-sun] Sun L., Romolini G., Dieu B., Grandjean D., Keshavarz M., Fron E., d'Acapito F., Roeffaers M.B.J., Van der Auweraer M., Hofkens J. - Ultrasensitive luminescence switching of zeolite Y confined silver clusters for dual-channel oxygen sensing Advanced Optical Materials 12, 2400784-1-2400784-12(2024)
33. [24-Vecc] Vecchi P., Ruani F., Mazzanti M., Loague Q.R., Mazzaro R., Boscherini F., Ventura B., Meyer G.J., Armaroli N., Caramori S., Pasquini L. - Impact of Co–Fe overlayers on charge carrier dynamics at WO3/BiVO4 heterojunctions: A picosecond-to-second spectroscopic analysis ACS Energy Letters 9, 2193-2200(2024)

34. [24-Virg] Virga S., Arrabito G., Ferrara V., Scopelliti M., Longo A., Pignataro B., Giannici F. - Bismuth drives the morphology and piezoresistivity of lead-free (TMSO)3Sn3xBi2(1−x)I9 halide perovskite thin films Journal of Materials Chemistry C 12, 12951-12961(2024)
35. [24-Xue] Xue X., Asenbauer J., Eisenmann T., Lepore G.O., d'Acapito F., Xing S., Tübke J., Mullaliu A., Li Y., Geiger D., Biskupek J., Kaiser U., Steinle D., Birrozzi A., Bresser D. - Exploration of the lithium storage mechanism in monoclinic Nb2O5 as a function of the degree of lithiation Small Structures 5, 2300545-1-2300545-11(2024) 1 citation
36. [23-Amat] Amatori S., López A., Meneghini C., Calcabrini A., Colone M., Stringaro A., Migani S., Khalakhan I., Iucci G., Venditti I., Battocchio C. - Gold nanorods derivatized with CTAB and hydroquinone or ascorbic acid: Spectroscopic investigation of anisotropic nanoparticles of different shapes and sizes Nanoscale Advances 5, 3924-3933(2023) 4 citations
37. [23-Bacc] Bacchella C., Camponeschi F., Kolkowska P., Kola A., Tessari I., Baratto M.C., Bisaglia M., Monzani E., Bubacco L., Mangani S., Casella L., Dell'Acqua S., Valensin D. - Copper binding and redox activity of α-synuclein in membrane-like environment Biomolecules 13, 287-1-287-19(2023) 7 citations
38. [23-Cama] Cámara F., Biagioni C., Ciriotti M.E., Bosi F., Kolitsch U., Paar W.H., Hålenius U., Lepore G.O., Blass G., Bittarello E. - Piccoliite, NaCaMn3+2(AsO4)2O(OH), a new arsenate from the manganese deposits of Montaldo di Mondovì and Valletta, Piedmont, Italy Mineralogical Magazine 87, 204-217(2023) 1 citation
39. [23-Chin] Chinnabathini V.C., Dingenen F., Borah R., Abbas I., van der Tol J., Zarkua Z., d'Acapito F., Nguyen T.H.T., Lievens P., Grandjean D., Verbruggen S.W., Janssens E. - Gas phase deposition of well-defined bimetallic gold-silver clusters for photocatalytic applications Nanoscale 15, 6696-6708(2023) 6 citations
40. [23-Ghor] Ghorbani E., Schiller M., Falk H.H., Wägele L.A., Eckner S., d'Acapito F., Scheer R., Albe K., Schnohr C.S. - Elucidating the local structure of V substitutes in In2S3 as potential intermediate band material by X-ray absorption spectroscopy and first principles calculations Journal of Physics: Energy 5, 035003-1-035003-14(2023)
41. [23-Goud] Goudjil M., Lepore G.O., Bindi L., Mugnaioli E., Baroni T., Mezaoui D., Bonazzi P. - Synthesis and characterization of AsO[(W,Mo)O3]13, a new (6)-intergrowth tungsten bronze (ITB) Journal of Solid State Chemistry 322, 123987-1-123987-7(2023) 1 citation
42. [23-Joub] Joubert J.M., Kalchev Y., Fantin A., Crivello J.C., Zehl R., Elkaïm E., Laplanche G. - Site occupancies in a chemically complex σ-phase from the high-entropy Cr–Mn–Fe–Co–Ni system Acta Materialia 259, 119277-1-119277-10(2023) 4 citations
43. [23-Laur] Laureti S., d'Acapito F., Imperatori P., Patrizi E., Varvaro G., Puri A., Cannas C., Capobianchi A. - Synthesis of highly ordered L10 MPt alloys (M = Fe, Co, Ni) from crystalline salts: An in situ study of the pre-ordered precursor reduction strategy Journal of Materials Chemistry C 11, 16661-16671(2023) 4 citations
44. [23-Meek] Meekel E.G., Schmidt E.M., Cameron L.J., Dharma A.D., Windsor H.J., Duyker S.G., Minelli A., Pope T., Lepore G.O., Slater B., Kepert C.J., Goodwin A.L. - Truchet-tile structure of a topologically aperiodic metal-organic framework Science 379, 357-361(2023) 2 citations
45. [23-Moni] Monico L., d'Acapito F., Cotte M., Janssens K., Romani A., Ricci G., Miliani C., Cartechini L. - Total electron yield (TEY) detection mode Cr K-edge XANES spectroscopy as a direct method to probe the composition of the surface of darkened chrome yellow (PbCr1-xSxO4) and potassium chromate paints Nuclear Instruments and Methods in Physics Research B 539, 141-147(2023) 2 citations
46. [23-Ritt] Ritter K., Gurieva G., Eckner S., Schwiddessen R., d'Acapito F., Welter E., Schorr S., Schnohr C.S. - Atomic scale structure and bond stretching force constants

in stoichiometric and off-stoichiometric kesterites Journal of Chemical Physics 159, 154705-1-154705-11(2023)

47. [23-Scar] Scaramuzza S., de Faria C.M.G., Coviello V., Forrer D., Artiglia L., Badocco D., Pastore P., Ghigna P., Postuma I., Cansolino L., Ferrari C., Bortolussi S., Vago R., Spinelli A.E., Bekic M., Colic M., Amendola V. - A laser synthesis route to boron-doped gold nanoparticles designed for X-ray radiotherapy and boron neutron capture therapy assisted by CT imaging Advanced Functional Materials 33, 2303366-1-2303366-15(2023) 4 citations
48. [23-Virg] Virga S., Longo A., Pipitone C., Giannici F. - Structural features governing the near-edge X-ray absorption spectra of lead halide perovskites Journal of Physical Chemistry C 127, 18058-18066(2023) 2 citations
49. [23-Xu] Xu M., Li Q., Song Y., Xu Y., Sanson A., Shi N., Wang N., Sun Q., Wang C., Chen X., Qiao Y., Long F., Liu H., Zhang Q., Venier A., Ren Y., d'Acapito F., Olivi L., de Souza D.O., Xin X., Chen J. - Giant uniaxial negative thermal expansion in $FeZr_2$ alloy over a wide temperature range Nature Communications 14, 4439-1-4439-8(2023) 8 Citations
50. [22-Berr] Berretti E., Pagliaro M.V., Giaccherini A., Montegrossi G., Di Benedetto F., Lepore G.O., d'Acapito F., Vizza F., Lavacchi A. - Experimental evidence of palladium dissolution in anodes for alkaline direct ethanol and formate fuel cells Electrochimica Acta 418, 140351-1-140351-9(2022) 8 citations
51. [22-Das] Das A., Balasubramanian C., Orpe P., Pugliese G.M., Puri A., Marcelli A., Saini N.L. - Morphological, electronic, and magnetic properties of multicomponent cobalt oxide nanoparticles synthesized by high temperature arc plasma Nanotechnology 33, 095603-1-095603-13(2022) 2 citations
52. [22-Fant] Fantin A., Cakir C.T., Kasatikov S., Schumacher G., Manzoni A.M. - Effects of heat treatment on microstructure, hardness and local structure in a compositionally complex alloy Materials Chemistry and Physics 276, 125432-1-125432-6(2022) 4 citations
53. [22-Kali] Kalinic B., Girardi L., Ragonese P., Faramawy A., Mattei G., Frasconi M., Baretta R., Bogialli S., Roverso M., Rizzi G.A., Maurizio C. - Diffusion-driven formation of Co_3O_4 nanopetals layers for photoelectrochemical degradation of organophosphate pesticides Applied Surface Science 596, 153552-1-153552-9(2022) 6 ciotations
54. [22-Koeb] Koeberl C., Glass B.P., Schulz T., Wegner W., Giuli G., Cicconi M.R., Trapananti A., Stabile P., Cestelli-Guidi M., Park J., Herzog G.F., Caffee M.W. - Tektite glasses from Belize, Central America: Petrography, geochemistry, and search for a possible meteoritic component Geochimica et Cosmochimica Acta 325, 232-257(2022) 4 citations
55. [22-Lepo] Lepore G.O., Checchia S., Baroni T., Brunelli M., d'Acapito F. - Outstation for X-ray powder diffraction at the Italian beamline at the European synchrotron Review of Scientific Instruments 93, 113903-1-113903-7(2022)
56. [22-Lepo1] Lepore G.O., Schingaro E., Mesto E., Lacalamita M., Cristiani C., Gallo Stampino P., Dotelli G., Finocchio E., d'Acapito F., Giuli G. - Lanthanum captured in montmorillonite: Evidence of inner-sphere complexes from X-ray Absorption Spectroscopy investigations Applied Clay Science 230, 106676-1-106676-7(2022) 6 citations
57. [22-Menu] Menushenkov A.P., Ivanov A.A., Chernysheva O.V., Rudnev I.A., Osipov M.A., Kaul A.R., Chepikov V.N., Mathon O., Monteseguro V., d'Acapito F., Puri A. - The influence of $BaSnO_3$ and $BaZrO_3$ nanoinclusions on the critical current and local structure of HTS coated conductors Superconductor Science and Technology 35, 065006-1-065006-9(2022) 5 citations
58. [22-Mich] Michez L.A., Petit M., Heresanu V., Le Thanh V., Prestat E., d'Acapito F., Ramasse Q., Boscherini F., Pochet P., Jamet M. - Unveiling the atomic position of C in $Mn_5Ge_3C_x$ thin films Physical Review Materials 6, 074404-1-074404-13(2022) 1 citation

59. [22-Moni] Monico L., Rosi F., Vivani R., Cartechini L., Janssens K., Gauquelin N., Chezganov D., Verbeeck J., Cotte M., d'Acapito F., Barni L., Grazia C., Buemi L.P., Andral J.L., Miliani C., Romani A. - Deeper insights into the photoluminescence properties and (photo)chemical reactivity of cadmium red (CdS1-xSex) paints in renowned twentieth century paintings by state-of-the-art investigations at multiple length scales European Physical Journal Plus 137, 311-1-311-21(2022) 9 citations
60. [22-Pipi] Pipitone C., Carlotto S., Casarin M., Longo A., Martorana A., Giannici F. - Bi3+ doping in 1D ((CH3)(3)SO)PbI3: A model for defect interactions in halide perovskites Journal of Materials Chemistry C 10, 1458-1469(2022)
61. [22-Pree] Preeti, Naidu K.L., Krishna M.G., Mohiddon M.A. - Investigation of crystallographic changes across the Cr/a-Si interface by X-ray absorption spectroscopy Applied Surface Science 592, 153204-1-153204-8(2022)
62. [21-Belt] Beltrami G., Di Renzo F., Parodi I., Alberti A., de Lourdes Guzman-Castillo M., Fajula F., Suard E., Martucci A. - Thermal activation of NH4 precursor of acidic omega zeolite: A neutron and in-situ synchrotron powder diffraction combined study Microporous and Mesoporous Materials 314, 110825-1-110825-12(2021)
63. [21-Frac] Fracchia M., Ghigna P., Marelli M., Scavini M., Vertova A., Rondinini S., Della Pergola R., Minguzzi A. - Molecular cluster route for the facile synthesis of a stable and active Pt nanoparticle catalyst New Journal of Chemistry 45, 11292-11303(2021) 7 citations
64. [21-Laur] Laureti S., Gerardino A., d'Acapito F., Peddis D., Varvaro G. - The role of chemical and microstructural inhomogeneities on interface magnetism Nanotechnology 32, 205701-1-205701-13(2021) 9 citations
65. [21-Marm] Marmiroli M., Pagano L., Rossi R., De la Torre-Roche R., Lepore G.O., Ruotolo R., Gariani G., Bonanni V., Pollastri S., Puri A., Gianoncelli A., Aquilanti G., d'Acapito F., White J.C., Marmiroli N. - Copper oxide nanomaterial fate in plant tissue: Nanoscale impacts on reproductive tissues Environmental Science and Technology 55, 10769-10783(2021) 20 citations
66. [21-Pugl] Pugliese G.M., Tortora L., Paris E., Wakita T., Terashima K., Puri A., Nagao M., Higashinaka R., Matsuda T.D., Aoki Y., Yokoya T., Mizokawa T., Saini N.L. - The local structure of the BiS2 layer in RE(O,F)BiS2 determined by in-plane polarized X-ray absorption measurements Physchem 1, 250-258(2021) 1 citation
67. [21-Puri] Puri A., Lepore G.O., Signorato R., Scarbolo P., Di Maio G., d'Acapito F. - The LISA CRG beamline at ESRF Springer Proceedings in Physics 220, 57-63(2021) In: "Synchrotron Radiation Science and Applications", Di Cicco A. (Eds.)Giuli G. (Eds.)Trapananti A. (Eds.)(Springer, 2021) pp.57-63 In: "2019 meeting of the Italian Synchrotron Radiation Society" - Camerino, Italy - 2019--09
68. [21-Vann] Vanni M., Bellini M., Borsacchi S., Calucci L., Caporali M., Caporali S., d'Acapito F., Geppi M., Giaccherini A., Ienco A., Manca G., Mio A.M., Nicotra G., Oberhauser W., Serrano-Ruiz M., Banchelli M., Vizza F., Peruzzini M. - Interlayer coordination of Pd-Pd units in exfoliated black phosphorus Journal of the American Chemical Society 143, 10088-10098(2021) 11 citations
69. [20-Biag] Biagioni C., Mauro D., Pasero M., Bonaccorsi E., Lepore G.O., Zaccarini F., Skogby H. - Crystal-chemistry of sulfates from the Apuan Alps (Tuscany, Italy). VI. Tl-bearing alum-(K) and voltaite from the Fornovolasco mining complex American Mineralogist 105, 1088-1098(2020) 7 citations
70. [20-Giacc] Giaccherini A., Griesi A., Montegrossi G., Romanelli M., Lepore G.O., Lavacchi A., Amthauer G., Redhammer G., Tippelt G., Martinuzzi S., Cucinotta G., Mannini M., Caneschi A., Di Benedetto F. - A new solvothermal approach to obtain nanoparticles in the Cu3SnS4-Cu2FeSnS4 join Journal of Geosciences 65, 3-14(2020) 5 citations
71. [20-Kesa] Kesavan J.K., d'Acapito F., Scardi P., Stavrinadis A., Agkul M.Z., Burgues-Ceballos I., Konstantatos G., Boscherini F. - Cation disorder and local structural distortions in AgxBi1–xS2 nanoparticles Nanomaterials 10, 316-1-316-13(2020) 4 citations

72. [20-Kuzn] Kuznetsov A.V., Churkin O.A., Popov V.V., Shchetinin I.V., Ivanov A.A., Yastrebtsev A.A., Gaynanov B.R., Yaroslavtsev A.A., Chernysheva O.V., Puri A., Alekseev P.A., Menushenkov A.P. - Magnetization of crystalline and amorphous phases of R2Ti2O7 and R2Zr2O7 (R = Gd, Dy, Tb) Journal of Superconductivity and Novel Magnetism 33, 2395–2404(2020) 5 citations
73. [20-Maur] Maurizio C., Mattarello V., Kalinic B., Michieli N., Balasa I.G., Scian C., Mattei G. - Structural modification of Au-Co thin films induced by annealing in oxidizing atmosphere Surface & Coatings Technology 385, 125309-1-125309-5(2020) 2 citations
74. [20-Maur2] Maurizio C., Michieli N., Kalinic B., Mattarello V., Scian C., Ciatto G., Mattei G. - Amorphous intermixing of noble and magnetic metals in thin film-based nanostructures Applied Surface Science 513, 145779-1-145779-8(2020) 1 citation
75. [20-Palu] Palumbo O., Manzi J., Meggiolaro D., Vitucci F.M., Trequattrini F., Curcio M., Paolone A., Brutti S. - Effect of transitional metals (Mn and Ni) substitution in LiCoPO4 olivines Molecules 25, 601-1-601-15(2020) 1 citation
76. [20-Pelli] Pelli Cresi J.S., Carlà F., Znaiguia R., Isérn H., Benedetti F., Gasperi G., Amidani L., Valeri S., Boscherini F., Luches P. - Structure of reduced cerium oxide ultrathin films on Pt(111): Local atomic environment and long-range order Advanced Materials Interfaces 7, 2000737-1-2000737-11(2020)
77. [20-Petr] Petroselli C., Moroni B., Crocchianti S., Selvaggi R., Soggia F., Grotti M., d'Acapito F., Cappelletti D. - Iron speciation in different Saharan dust advections and effect of the procedural blank on the results from X-ray absorption spectroscopy and selective leaching experiments Atmosphere 11, 735-1-735-14(2020) 1 citation
78. [20-Popo] Popov V.V., Menushenkov A.P., Ivanov A.A., Yastrebtsev A.A., Gaynanov B.R., d'Acapito F., Puri A. - A XAFS investigation of amorphous-to-crystalline and fluorite-to-pyrochlore phase transitions in Ln2M2O7 (Ln = Gd, Tb, Dy; M = Ti, Zr) Radiation Physics and Chemistry 175, 108469-1-108469-5(2020) 12 citations
79. [20-Righ] Righi L., Merlini M., Gemmi M. - High-temperature evolution of the incommensurate composite crystal Ca0.83CuO2 Crystals 10, 630-1-630-11(2020) 1 citation
80. [20-Sche] Scherb T., Fantin A., Checchia S., Stephan-Scherb C., Escolástico S., Franz A., Seeger J., Meulenberg W.A., d'Acapito F., Serra J.M. - Unravelling the crystal structure of Nd5.8WO12-δ and Nd5.7W0.75Mo0.25O12-δ mixed ionic electronic conductors Journal of Applied Crystallography 53, 1471-1483(2020) 2 citations
81. [20-Soff] Soffientini A., Ghigna P., Spinolo G., Boldrini S., Famengo A., Tamburini U.A. - Nanostructured calcium cobalt oxide Ca3Co4O9 as thermoelectric material. Effect of nanostructure on local coordination, Co charge state and thermoelectric properties Journal of Physics and Chemistry of Solids 143, 109474-1-109474-10(2020) 8 citations
82. [20-Verd] Verdy A., d'Acapito F., Dory J.B., Navarro G., Bernard M., Noé P. - Effect of nitrogen on the amorphous structure and subthreshold electrical conduction of GeSeSb-based ovonic threshold switching thin films Physica Status Solidi-Rapid Research Letters 14, 1900548-1-1900548-7(2020) 10 citations
83. [20-Visi] Visibile A., Fracchia M., Baran T., Vertova A., Ghigna P., Ahlberg E., Rondinini S., Minguzzi A. - Electrodeposited Cu thin layers as low cost and effective underlayers for Cu2O photocathodes in photoelectrochemical water electrolysis Journal of Solid State Electrochemistry 24, 339-355(2020) 7 citations

Grenoble, May 28 2025